

INFORMATION TO USERS

This reproduction was made from a copy of a document sent to us for microfilming. While the most advanced technology has been used to photograph and reproduce this document, the quality of the reproduction is heavily dependent upon the quality of the material submitted.

The following explanation of techniques is provided to help clarify markings or notations which may appear on this reproduction.

1. The sign or "target" for pages apparently lacking from the document photographed is "Missing Page(s)". If it was possible to obtain the missing page(s) or section, they are spliced into the film along with adjacent pages. This may have necessitated cutting through an image and duplicating adjacent pages to assure complete continuity.
2. When an image on the film is obliterated with a round black mark, it is an indication of either blurred copy because of movement during exposure, duplicate copy, or copyrighted materials that should not have been filmed. For blurred pages, a good image of the page can be found in the adjacent frame. If copyrighted materials were deleted, a target note will appear listing the pages in the adjacent frame.
3. When a map, drawing or chart, etc., is part of the material being photographed, a definite method of "sectioning" the material has been followed. It is customary to begin filming at the upper left hand corner of a large sheet and to continue from left to right in equal sections with small overlaps. If necessary, sectioning is continued again—beginning below the first row and continuing on until complete.
4. For illustrations that cannot be satisfactorily reproduced by xerographic means, photographic prints can be purchased at additional cost and inserted into your xerographic copy. These prints are available upon request from the Dissertations Customer Services Department.
5. Some pages in any document may have indistinct print. In all cases the best available copy has been filmed.

**University
Microfilms
International**

300 N. Zeeb Road
Ann Arbor, MI 48106

8323264

Atsina, Komli-Kofi

**ISOMETRIC RESPONSES OF RAT EXTENSOR DIGITORUM LONGUS AND
SOLEUS NEUROMUSCULAR SYSTEMS TO ABNORMAL EXTRACELLULAR
CALCIUM AND MAGNESIUM CONCENTRATIONS**

Iowa State University

PH.D. 1983

**University
Microfilms
International** 300 N. Zeeb Road, Ann Arbor, MI 48106

PLEASE NOTE:

In all cases this material has been filmed in the best possible way from the available copy. Problems encountered with this document have been identified here with a check mark .

1. Glossy photographs or pages _____
2. Colored illustrations, paper or print _____
3. Photographs with dark background _____
4. Illustrations are poor copy _____
5. Pages with black marks, not original copy _____
6. Print shows through as there is text on both sides of page _____
7. Indistinct, broken or small print on several pages
8. Print exceeds margin requirements _____
9. Tightly bound copy with print lost in spine _____
10. Computer printout pages with indistinct print _____
11. Page(s) _____ lacking when material received, and not available from school or author.
12. Page(s) _____ seem to be missing in numbering only as text follows.
13. Two pages numbered _____. Text follows.
14. Curling and wrinkled pages _____
15. Other Dissertation contains pages with print at a slant, filmed as received.

University
Microfilms
International

Isometric responses of rat extensor digitorum longus and
soleus neuromuscular systems to abnormal extracellular
calcium and magnesium concentrations

by

Komli-Kofi Atsina

A Dissertation Submitted to the Graduate
Faculty in Partial Fulfillment of the
Requirements for the Degree of

DOCTOR OF PHILOSOPHY

Major: Biomedical Engineering

Approved:

Signature was redacted for privacy.

In Charge of Major Work

Signature was redacted for privacy.

Professor-in-charge,
Biomedical Engineering Program

Signature was redacted for privacy.

For the Graduate College

Iowa State University
Ames, Iowa

1983

TABLE OF CONTENTS

	Page
LIST OF SYMBOLS AND ABBREVIATIONS	vii
INTRODUCTION	1
LITERATURE REVIEW	3
Background to Neuromuscular Activity	3
Calcium and Magnesium Effects	5
Muscle Characteristics	9
Labile Nature of Neuromuscular Transmission	14
MATERIALS AND METHODS	19
RESULTS AND DISCUSSIONS	32
Perfusion Techniques	32
Control Data #1: Intact Animal	36
Control Data #2: Normal Krebs Perfusion	39
Modified Krebs #1: Decreased $[Ca^{++}]$ and Normal $[Mg^{++}]$	42
Modified Krebs #2: Decreased $[Ca^{++}]$ and Increased $[Mg^{++}]$	45
Modified Krebs #3: Decreased $[Mg^{++}]$ and Normal $[Ca^{++}]$	48
Modified Krebs #4: Decreased $[Mg^{++}]$ and Decreased $[Ca^{++}]$	52
Stimulus Threshold Voltages	59
Tetanic Contractions	60
Effect of Insulin	74
CONCLUSIONS	81
BIBLIOGRAPHY	84
ACKNOWLEDGEMENTS	89

LIST OF TABLES

	Page
Table 1. Data from muscles with intact vascular system	38
Table 2a. Data from muscles perfused with normal Krebs	41
Table 2b. Ionic levels of the influent normal Krebs	41
Table 2c. Ionic levels of the effluent normal Krebs	41
Table 3a. Data from muscles perfused with modified Krebs #1	44
Table 3b. Ionic levels of the influent modified Krebs #1	44
Table 3c. Ionic levels of the effluent modified Krebs #1	44
Table 4a. Data from muscles perfused with modified Krebs #2	47
Table 4b. Ionic levels of the influent modified Krebs #2	47
Table 4c. Ionic levels of the effluent modified Krebs #2	47
Table 5a. Data from muscles perfused with modified Krebs #3	50
Table 5b. Ionic levels of the influent modified Krebs #3	50
Table 5c. Ionic levels of the effluent modified Krebs #3	50
Table 6a. Data from muscles perfused with modified Krebs #4	54
Table 6b. Ionic levels of the influent modified Krebs #4	54
Table 6c. Ionic levels of the effluent modified Krebs #4	54
Table 7a. Reaction of EDL at 0.4 pps to different calcium and magnesium levels in Krebs solution	55
Table 7b. Net ionic gain (+) or loss (-) in Krebs solution during EDL perfusion	55
Table 8a. Reaction of SOL at 0.1 pps to different calcium and magnesium levels in Krebs solution	56
Table 8b. Net ionic gain (+) or loss (-) in Krebs solution during SOL perfusion	56

	Page
Table 9. Sample values of pH, pCO ₂ and pO ₂ for the perfused Krebs solution	57
Table 10. Perfusion pressure values at optimal flowrates of Krebs solution	58
Table 11a. Reaction of EDL at 0.4 pps to different [Ca ⁺⁺] and [Mg ⁺⁺] in Krebs solution containing 0.5 mg/l of insulin	75
Table 11b. Ionic changes in "insulinated" Krebs during EDL perfusion	75
Table 12a. Reaction of SOL at 0.1 pps to different [Ca ⁺⁺] and [Mg ⁺⁺] in Krebs solution containing 0.5 mg/l of insulin	76
Table 12b. Ionic changes in "insulinated" Krebs during SOL perfusion	76
Table 13. Sample values of pH, pCO ₂ and pO ₂ for the "insulinated" Krebs solution	79

LIST OF FIGURES

	Page
Figure 1. Stimulation and data acquisition processes	20
Figure 2. Control sequence of the infusion process	21
Figure 3. Sample tracings from muscles with intact vascular bed	37
Figure 4. Sample tracings from muscles perfused with normal Krebs	40
Figure 5. Sample tracings from muscles perfused with modified Krebs #1	43
Figure 6. Sample tracings from muscles perfused with modified Krebs #2	46
Figure 7. Sample tracings from muscles perfused with modified Krebs #3	49
Figure 8. Sample tracings from muscles perfused with modified Krebs #4	53
Figure 9. Sample tetanic tracings from EDL muscle with intact vascular bed	62
Figure 10. Sample tetanic tracings from EDL muscle perfused with normal Krebs solution	63
Figure 11. Sample tetanic tracings from EDL muscle perfused with modified Krebs #1	64
Figure 12. Sample tetanic tracings from EDL muscle perfused with modified Krebs #2	65
Figure 13. Sample tetanic tracings from EDL muscle perfused with modified Krebs #3	66
Figure 14. Sample tetanic tracings from EDL muscle perfused with modified Krebs #4	67
Figure 15. Sample tetanic tracings from SOL muscle with intact vascular bed	68

	Page
Figure 16. Sample tetanic tracings from SOL muscle perfused with normal Krebs	69
Figure 17. Sample tetanic tracings from SOL muscle perfused with modified Krebs #1	70
Figure 18. Sample tetanic tracings from SOL muscle perfused with modified Krebs #2	71
Figure 19. Sample tetanic tracings from SOL muscle perfused with modified Krebs #3	72
Figure 20. Sample tetanic tracings from SOL muscle perfused with modified Krebs #4	73

LIST OF SYMBOLS AND ABBREVIATIONS

ACh	Acetylcholine
AChE	Acetylcholinesterase
ADP	Adenosine diphosphate
AP	Action potential
ATP	Adenosine triphosphate
ATPase	Adenosine triphosphatase
Corning 7	Corning Glass Works, pH meter model 7
CT	Control experiment
C10	Decamethonium
DF-596	Competitive ACh antagonist
dl	Deciliter
dTc	d-Tubocurarine
ECF	Extracellular fluid
EDL	Extensor digitorum longus
EDTA	Ethylene diaminetetraacetate
EPP	Endplate potential
F-actin	Fibrous actin
FR	Optimal flowrate
FT10C	Grass Instrument Co., force transducer model FT10C
gastroc	Gastrocnemius
Grass 5	Grass Instrument Co., polygraph model 5
Hz	Hertz
IL 343	Instrumentation Laboratory Co., flame photometer model 343

IL 513	Instrumentation Laboratory Co., pH/blood gas analyzer model 513
MAP	Muscle action potential
MEPP	Miniature endplate potential
meq	Milliequivalent
MK	Modified Krebs solution
mN	Millinewton
NADH	Dihyronicotinamide adenine dinucleotide
NMJ	Neuromuscular junction
NMS	Neuromuscular system
°C	Degree centigrade
PP	Perfusion pressure
RF	Radio frequency
ROTOCHEM IIA	Worthington Instruments, spectrometer model ROTOCHEM IIA
rt	Right
SDH	Succinic dehydrogenase
SIU5	Grass Instrument Co., stimulus isolation unit model SIU5
SOL	Soleus
SR	Sarcoplasmic reticulum
stim	Stimulation
S88	Grass Instrument Co., stimulator model S88
Tc	Rectal temperature
Ts	Krebs solution temperature
T10	Interval between start of occlusion and start of perfusion
T30	Interval between start of occlusion and end of 20 min of perfusion

T50	Interval between start of occlusion and end of 40 min of perfusion
wt	Weight
WZIRO31	Cole-Parmer Instruments Co., pump controller unit model WZIRO31
[]	Concentration of an ion
[] _e	Extracellular concentration of an ion
[] _i	Intracellular concentration of an ion
43TD	Yellow Springs Instrument Co., telethermometer model 43TD
Corning 920M	Corning Glass Works, chloride meter model 920M

INTRODUCTION

The main objective of the research described in this dissertation was to determine whether differences in nerve, muscle, and neuromuscular junction (NMJ) could result in varying responses to abnormal calcium and magnesium concentrations ($[Ca^{++}]$, $[Mg^{++}]$). To this end, the hypothesis that different extracellular concentrations of calcium and magnesium ($[Ca^{++}]_e$, $[Mg^{++}]_e$) have quantitatively different effects on isometric responses of slow muscles, as represented by soleus (SOL), and fast muscles, as represented by extensor digitorum longus (EDL) of the rat was tested.

Four different combinations of altered $[Ca^{++}]_e$ and $[Mg^{++}]_e$ were tested to determine whether, at a particular concentration, transmission would be affected more in one type of NMJ than in the other. Isometric twitch and tetanic tensions were recorded in response to nerve and muscle stimulation. Furthermore, stimulus threshold voltages were monitored to indicate whether these changes in $[Ca^{++}]_e$ and $[Mg^{++}]_e$ would affect the thresholds of one nerve-muscle preparation more than the other.

The hypothesis was inferred from several findings in the literature concerning the physiological roles played by Ca^{++} and Mg^{++} in regulating the functional integrity of the neuromuscular system (NMS), and the structural, physiological and chemical characteristics of the SOL and EDL muscles.

The SOL NMJ is known to have a lower safety factor than the EDL NMJ (Paton and Waud, 1967). This should make the SOL NMJ more sensitive to altered Ca^{++} and Mg^{++} levels than the EDL NMJ.

The neurons to SOL muscles discharge at low frequencies (10-20 Hz) for sustained periods while the neurons to EDL muscles discharge at higher frequencies (30-60 Hz) for brief periods (Eccles et al., 1958). Since the EDL isometric tension decreases dramatically after a few stimuli at more than 3 Hz (preliminary observation), it was thought possible that at certain ionic levels and frequencies of stimulation the decrease in response would be greater in the EDL than in the SOL, that fatigue of the NMJ would offset the safety factor advantage the EDL normally possesses.

The alpha motorneurons to the SOL muscles are smaller than those to the EDL. Smaller neurons with their higher input resistance are more easily excited by synaptic potentials (Henneman et al., 1965), but the thresholds of their axons for extracellularly applied current are higher than for larger axons.

Comparison of the isometric tensions for the two neuromuscular systems, using normal and altered $[Ca^{++}]_e$ and $[Mg^{++}]_e$, indicated a different sensitivity to changes in $[Ca^{++}]_e$ and $[Mg^{++}]_e$. Single twitch tension appeared to be affected less in the EDL than in the SOL NMS; tetanic tension appeared to be affected more in the EDL than in the SOL. No consistent effects on threshold voltages were observed.

LITERATURE REVIEW

Background to Neuromuscular Activity

During early embryogenesis, nerve cells and muscle fibers develop independently. They become dependent on each other only after they have acquired to a certain degree those specific properties that allow them to interact with each other, that is, the ability of the nerve terminal to synthesize and release acetylcholine (ACh), as well as that of the muscle to respond to the released ACh (Kullberg et al., 1977).

The initial input to the control sequence of muscular contraction is the passage of a nerve impulse (AP) along a motor nerve and its branches to the muscle fibers. The arrival of the nerve AP at the motor endplate causes a large transient synchronous release of ACh quanta within about 1 msec (Katz, 1971). The ACh then diffuses across the narrow (about 50 nm) synaptic cleft to cause a large depolarization called the endplate potential (EPP), which in turn depolarizes the muscle membrane sufficiently to initiate a propagated muscle action potential (MAP) (Lester, 1977).

The removal of ACh from the endplate region occurs both by diffusion and by hydrolysis catalyzed by the enzyme acetylcholinesterase (AChE). The resulting choline is taken up by the nerve terminal and re-acetylated in the presence of the enzyme choline acetyltransferase.

The muscle membrane potential (MAP) spreads inward along the transverse tubular system and triggers the release of Ca^{++} from the terminal

cisternae of the sarcoplasmic reticulum (SR) raising free ionized $[Ca^{++}]_i$ from 10^{-7} M to about 10^{-5} M. The increased $[Ca^{++}]_i$ initiates contraction (Ebashi and Endo, 1968). Ca^{++} binds to troponin-C on the thin filaments of F-actin. This alters the calcium-troponin-tropomyosin-actin complex to permit the tropomyosin to move laterally. This movement uncovers the binding sites for the myosin heads and removes the suppression of the actin stimulation of magnesium-activated myosin ATPase activity. A pre-existing ADP-orthophosphate-myosin complex located in the cross-bridges of the thick filaments combines with the available actin site to form acto-myosin and an active ATPase. The ATP already hydrolyzed on myosin by myosin ATPase is released as ADP and orthophosphate, and an impulsive transient force is developed by the cross-bridge complex of the contractile proteins, actin and myosin. This unitary mechanical response or twitch constitutes the end of skeletal muscle contraction (Ebashi and Endo, 1968).

Relaxation of the muscle commences with the uptake of Ca^{++} by the SR. As more Ca^{++} is pumped into the SR, more Ca^{++} is released from the contractile protein complex until free ionized $[Ca^{++}]_i$ is lower than 10^{-7} M. Troponin-I inhibition of actin-myosin cross-link formation is restored. As cross-links break and myosin-ATP complex is formed, the tension-developing state decays. Myosin-ADP-orthophosphate complex is reformed to restore the initial resting state of the muscle (Ebashi et al., 1969; Huxley, 1974).

Calcium and Magnesium Effects

The dependence of neuromuscular function on $[Ca^{++}]_e$ cannot be over-emphasized. Each of the various processes from nerve activation to muscle mechanical response is affected to a certain degree by $[Ca^{++}]_e$. $[Ca^{++}]_e$ influences the initiation of the nerve AP and its propagation along the axon (Frankenhaeuser, 1957), the coupling between the depolarization of the nerve terminal by the AP and the secretion of transmitter (Katz and Miledi, 1965), the interaction between ACh and the postsynaptic membrane (Takeuchi, 1963; Nastuk and Liu, 1966), and finally, the depolarization-contraction coupling in muscle, followed by the contraction of the skeletal muscle.

$[Ca^{++}]_e$ exerts a critical influence on membrane excitability. Although moderate elevations of Ca^{++} level in the ECF may have no clinically detectable influences on these tissues, extreme hypercalcaemia increases the threshold for excitation of nerve and muscle. In contrast, modest diminution in the level of free, ionized Ca^{++} may decrease the thresholds of excitation in a striking fashion, leading to tetanic seizures due to increased activity of the motor nerve fibers. It is believed that Ca^{++} exerts its effect by regulating the cell-membrane permeability to Na^+ and K^+ : increased $[Ca^{++}]_e$ diminishes the permeability of the cell, while decreased $[Ca^{++}]_e$ augments permeability (Erulkar and Fine, 1979).

In addition, the increase in the rate of transmitter release by the presynaptic AP depends on the presence of Ca^{++} ions in the ECF. In the absence of Ca^{++} ions, stimulation of the motor nerve produces no EPP.

According to Rahamimoff (1976), this lack of response to nerve stimulation is not due to lack of invasion of the electrical signal into the nerve terminals, for in 1965, Katz and Miledi, using focal extracellular recording from the motor nerve terminal, observed that in the absence of $[Ca^{++}]_e$ the AP is still able to invade terminals, but fails to induce release of transmitter. From the above findings, Rahamimoff (1976) concludes that the activation of the secretion process is the main calcium-requiring process in the formation of the EPP which must exceed the electrical threshold of the muscle membrane to create an AP in the muscle.

Mg^{++} is a cofactor of all enzymes involved in phosphate transfer reactions that utilize ATP and other nucleotide triphosphates as substitutes. But it also plays an important role with regard to neuromuscular transmission and muscular excitability. Abnormally low $[Mg^{++}]$ in the ECF results in increased ACh release and increased muscle excitability that can produce tetany (Jenkinson, 1957). Conversely, excess $[Mg^{++}]$ causes a decrease in ACh release by motor nerve impulses, reduces the sensitivity of the motor endplate to applied ACh, and decreases the amplitude of the EPP. The most critical of these effects is inhibition of ACh release (Hubbard, 1973). The effects of elevated Mg^{++} , which is a competitive antagonist to Ca^{++} in transmitter release (Jenkinson, 1957), is to interfere with and progressively block the presynaptic release of ACh. $[Mg^{++}]$ exhibits effects on neuron excitability similar to those of $[Ca^{++}]$, only less in potency (Erulkar and Fine, 1979; Rahamimoff, 1976).

Although the actions of Ca^{++} and Mg^{++} are synergistic as far as influencing the excitability of nerve membranes is concerned, they are an-

tagonistic in initiating transmitter release (Jenkinson, 1957). A reduction of $[Ca^{++}]$ in the endplate region causes a neuromuscular block by decreasing the number of ACh quanta released by the nerve AP (Katz and Miledi, 1965). Mg^{++} antagonizes the effect of Ca^{++} ; an increase in $[Mg^{++}]$ in the presence of normal $[Ca^{++}]$ inhibits ACh release (Katz and Miledi, 1967b).

Katz and Miledi (1965; 1967b) are generally credited with determining the way Ca^{++} is currently perceived to act in synaptic transmission. The nerve terminal contains special intracellular vesicles filled with the transmitter substance. When the neuron is in the resting state, the membrane is relatively impermeable to Ca^{++} ions, which have a much higher concentration outside the cell than inside. Depolarization opens Ca^{++} channels in the presynaptic terminal membrane; as a result the ions flow inward, propelled by the electrochemical gradient arising from what remains of the electrical potential across the membrane as well as the lesser concentration of Ca^{++} inside the terminal. The consequent rise in $[Ca^{++}]_i$, the intraterminal free $[Ca^{++}]$, induces the fusion of the synaptic vesicle membrane with the terminal membrane by an unknown mechanism; the vesicular contents are then extruded into the synaptic cleft.

Originally, Katz and Miledi (1965; 1967b) formulated their results as a hypothesis after they showed that transmitter release from the NMJ could be triggered by focal current pulses without nerve impulses, and that this release occurred only when Ca^{++} was present at the time of depolarization. Subsequently, however, Katz and Miledi (1967a; 1969) verified their hypothesis through experimentation on the squid giant

synapse. They found that depolarization of tetrodotoxin-blocked (Na^+ channel-blocked) terminals sufficed to trigger an increase in Ca^{++} conductance and release of neurotransmitter. Thus, Na^+ influx did not appear to be essential for transmitter release. The magnitude of the depolarization-induced inward current and the amount of transmitter release depended upon the $[\text{Ca}^{++}]$ in the bathing medium; depolarization to a membrane potential near the Ca^{++} equilibrium potential suppressed both inward current and the transmitter release.

Further support for the Ca^{++} hypothesis came from the work of Llinas and Nicholson (1975), who employed the Ca^{++} sensitive photoprotein, aequorin, to demonstrate directly the association between the rise in $[\text{Ca}^{++}]_i$ and transmitter release. They injected aequorin into the squid presynaptic terminals and measured the depolarization-induced increase in $[\text{Ca}^{++}]_i$ by the increased light output. Furthermore, Miledi (1973) showed that iontophoresis of Ca^{++} , but not Mg^{++} , into the squid presynaptic terminal triggered transmitter release without depolarization, proving beyond any reasonable doubt that a rise in $[\text{Ca}^{++}]_i$ is necessary and sufficient to trigger the release of neurotransmitters.

Both Ca^{++} and Mg^{++} are known to have specific effects on blood vessels. An increase in $[\text{Ca}^{++}]$ results in vasoconstriction since Ca^{++} stimulates smooth muscle contraction. Conversely, an increase in $[\text{Mg}^{++}]$ causes powerful vasodilation because Mg^{++} inhibits the smooth muscles of blood vessels (Stainsby, 1973).

Muscle Characteristics

On the basis of differences in time course of the isometric twitch, three kinds of motor units have been distinguished in the rat (Close, 1967) and these have been referred to as fast, intermediate, and slow units. Intermediate and slow motor units have been found in SOL muscles whereas EDL is virtually homogeneous and composed almost entirely of fast units. Close (1967) also showed that only about one in ten SOL motor units is an intermediate unit and that the characteristics determined from contractions of whole SOL muscles are very nearly the same as the average values obtained for slow units.

Buchthal and Schmalbruch (1980) also indicated two types of red muscle fibers in the mixed SOL muscle of the rat. They distinguished between them on the basis of contraction time and histochemical properties. The faster twitch fibers stained intensely for oxidative enzymes (SDH and NADH) as did the slower twitch fibers. This implies that they are both resistant to fatigue. The faster twitch fibers stained more intensely for ATPase at pH 9.4. This type of staining is also found in easily fatigued fast twitch fibers and is characteristic of rapid contraction. These fast twitch, fatigue-resistant fibers in the rat have been named superfibers.

Morphologically (Padykula and Gauthier, 1967), the slow SOL muscle can be distinguished by its redder color, due to its large content of mitochondrial cytochrome and myoglobin and its high capillary density, from the fast EDL muscle which appears paler (white) as a result of its

low capillarization as well as its low content of myoglobin and mitochondrial cytochrome.

In a review article, Close (1972) cited Ranvier (1873) as the first to show that muscles which consist of slow twitch fibers have more capillaries than muscles composed mainly of fast twitch fibers. In the soleus muscle of the cat the total capacity of blood flow is 2.5 times greater than in the gastrocnemius (gastroc) (Folkow and Halicka, 1968). A similar difference exists in the total surface area of the capillaries per cross-sectional area of the muscle. In the cat when peripheral resistance is decreased by close arterial injection of ACh the blood through the SOL will flow at a rate of 263 ml/min/100 g whereas only 95 ml/min/100 g of blood will flow through the gastroc (Hilton et al., 1970). Folkow and Halicka (1968) related the blood flow in the gastroc and SOL muscles of the cat to the O_2 consumption per twitch and to the rate of activation; the maximum blood flow is larger and the O_2 consumption per twitch is lower in SOL than in gastroc muscle. Therefore, the blood supply can deliver the O_2 needed to sustain the SOL muscle up to an activation frequency of about 20 Hz. In the gastroc muscle the blood flow is less, the O_2 consumption is higher, the capacity for delivery fails at a low rate of activation (about 4 Hz), and the fibers switch to anaerobic metabolism. Also, in the rat the blood supply is more extensive in slow SOL muscles than it is in fast EDL (Andrew and Part, 1972).

SOL muscle fibers are thin, possess broad Z-lines, and are rich in lipid droplets; the EDL muscle fibers, on the other hand, are thick, have narrow Z-lines, and are poor in fat droplets. Also, the number of cross-

bridges constituting the M-line is greater in fast than in slow twitch fibers, presumably to insure the stability of the filaments required during the fast twitch (Buchthal and Schmalbruch, 1980). In addition, the incidence of triadic junctions and the volume of the muscle fiber occupied by T-tubules and their terminal cisternae are lower in slow twitch than in fast twitch fibers (Luff and Atwood, 1971). In their review of mammalian motor units, Buchthal and Schmalbruch (1980) stated that the maximum rate of Ca^{++} uptake by SR is five to six times faster in fast than in slow muscle as a result of the higher content of SR in fast than in slow twitch muscle, implying that a fast twitch muscle has a shorter relaxation time than a slow one.

Studies of the dynamic properties (Close, 1972) of the two types of muscles have shown that the SOL whole muscle responds to stimulus with a slow twitch (maximum shortening velocity: 17 mm/sec), whereas the EDL shows a fast twitch response (maximum shortening velocity: 42 mm/sec) to an impulse. The SOL whole muscle has the ability to sustain activities for long periods (tonic activities), displays an easy fusion of tetanic responses at low frequencies (about 10 Hz), and is more resistant to fatigue; the EDL whole muscle, on the other hand, can sustain activities sporadically for short periods (phasic activities), will yield to tetanic responses only at high frequencies (about 40 Hz) of stimulation, and shows less resistance to fatigue.

The nerve fibers innervating the SOL muscles are small in diameter and they terminate in grapelike clusters as opposed to the EDL's larger nerve fibers with plaquelike terminations. These terminals in the SOL

muscles are apposed by shallow irregular junctional folds to form a simple NMJ; on the other hand, the bulblike nerve terminal expansions of the EDL fibers are apposed by deeper regular junctional folds to form a complex NMJ (Ellisman et al., 1976).

Ultrastructurally, Padykula and Gauthier (1970) have established distinct differences among NMJs of red, white, and intermediate fibers of the albino rat diaphragm. In the red fiber the neuromuscular relationship presents the least sarcoplasmic and axoplasmic surface at each contact. Points of contact are relatively discrete and separate, and axonal terminals are small and elliptical. The junctional folds are relatively shallow, sparse, and irregular in arrangement. Axoplasmic vesicles are moderate in number, and sarcoplasmic vesicles are sparse. In the white fiber, flat axonal terminals present considerable axoplasmic surface. Vast sarcoplasmic surface area is created by long, branching, closely spaced junctional folds that may merge with folds at adjacent contacts to occupy a more continuous and widespread area. Axoplasmic and sarcoplasmic vesicles are numerous. Both axoplasmic and sarcoplasmic mitochondria of the white fiber usually contain intramitochondrial granules. The intermediate fiber has large axonal terminals that are associated with the most widely spaced and deepest junctional folds. In all three fibers, the junctional sarcoplasm is rich in free ribosomes, cisternae of granular endoplasmic reticulum, and randomly distributed microtubules.

A distinctive cytochemical property of the sarcoplasmic surface is the presence of AChE (Salpeter, 1967), and it is possible that the amount of membrane surface might reflect differences in this enzymatic activity

among the three fiber types. Also, the abundance of axoplasmic vesicles (in addition to a highly invaginated sarcoplasmic membrane) in the white fiber might reflect a potentially greater supply of ACh or some trophic factor. Moreover, the sarcoplasmic reticulum, as well as the intra-mitochondrial granules which occur most frequently in both the axoplasmic and sarcoplasmic mitochondria of the white fiber, are known to be sites for concentrating cations (Thomas and Greenawalt, 1968); the possibility exists that $[Ca^{++}]_i$ can be reduced faster at the NMJ of the white fiber.

According to Ellisman et al. (1976), the size of the NMJ has been shown to be proportional to the diameter of the muscle fiber and to the frequency of spontaneous MEPPs. Despite the gross morphological differences in endplate structure visualized at relatively low magnifications in thin sections, rat EDL and SOL fibers cannot be distinguished on the basis of size, number, or distribution of molecular specializations of the pre- and post synaptic junctional membranes exposed by freeze fracturing.

Size differences in motor neurons suggest differences in such properties as rate of discharge and conduction velocity. It is generally accepted that the conduction velocity is directly related to fiber diameter and to internodal distance (Gasser and Grundfest, 1939). In cat, the alpha motor neurons to the slow SOL muscle have a mean diameter which is about 78% of the diameter of those innervating the fast gastroc (Eccles and Sherrington, 1930). The alpha motor fibers to the SOL discharge at lower frequencies (10-20 times/sec) than those supplying fast muscles (30-60 times/sec) (Eccles et al., 1958).

The transmembrane potential is higher in fast twitch muscle fibers than in slow twitch (Hanson, 1974). In cat (Buller et al., 1965) and in humans (Buchthal et al., 1973), the rise time of the AP has been found to be shorter in fast than in slow twitch muscle fibers. In the fast twitch muscle fibers the sensitivity to ACh is confined to the region of the endplates; in slow twitch fibers there is also a low sensitivity to ACh over the entire area of the membrane (Miledi and Zelena, 1966).

The effect of temperature on contraction time has also been studied by Close and Hoh (1968). In the rat, the contraction time of slow twitch fibers decreases more with increasing temperature than that of fast twitch fibers.

According to Buchthal and Schmalbruch (1970; 1980) circulatory arrest due to or producing anoxia eliminates the responses of fibers with long contraction times in a mixed muscle. Hence, slow twitch muscle fibers are more susceptible to lack of O_2 than fast twitch fibers, in which metabolism is mainly anaerobic.

Labile Nature of Neuromuscular Transmission

Paton and Waud (1967) reported that a margin of safety exists for transmission at the neuromuscular synapse, that is, the EPP is more than adequate to trigger a propagated response over a wide range of frequencies of excitation. They derived a physiological parameter, the safety factor for transmission, to determine the extent of interference with synaptic mechanisms that can exist without failure of transmission. They assessed

the safety factor postsynaptically by determining the relationship between the receptor capacity available and that necessary for transmission. In this method, the receptor pool was reduced until the activity achieved within it by a normal transmitter output fell to threshold. Applying graded doses of suitable stimulants (succinylcholine, decamethonium, octamethonium or iodo-choline) and competitive antagonists (tubocurarine, gallamine or DF-596), they were able to determine the degree of receptor occlusion produced by the antagonist at any given degree of neuromuscular block. Their method was based on the assumption that the rapidly destructible ACh and the more stable depolarizing agents act by identical mechanisms at the same endplate receptors and are therefore antagonized to the same extent by a drug such as tubocurarine. To determine the degree of receptor occlusion, the dose ratio method (Gaddum et al., 1955) was used. The principle consists of finding the ratio in which the dose of a stimulant must be increased in the presence of an antagonist in order to match a control response.

The safety factor for transmission (a ratio of EPP amplitude to threshold depolarization) was given as 1.8 for SOL and 2-3.7 for EDL. They hypothesized that the lower safety factor in the SOL may represent a compromise between reliability of synaptic transmission and necessity to maintain prolonged tetanic release of transmitter; the higher safety factor in EDL insures a reliable initial force of contraction because EDL whole muscle, like all fast muscles, is for swift motions.

Studies in the cat (Jewell and Zaimis, 1954) have shown that the SOL whole muscle (a slow muscle) and the tibialis anterior (a fast muscle) differ in their sensitivity to neuromuscular blocking agents. Whereas,

tibialis is very sensitive to decamethonium (C10) SOL is particularly resistant, and although both muscles are sensitive to d-Tubocurarine (dTc), SOL is the more sensitive of the two (Paton and Zaimis, 1951). The C10 block in tibialis is due to depolarization, and the block in the SOL is initially the result of a depolarization which is manifest before its curare-like action (competitive antagonism) becomes established. In other words, in tibialis (a white muscle) C10 acts as a depolarizing substance causing tibialis to exhibit a slowly decreasing sensitivity to C10. But in SOL (a red muscle) the C10 exhibits a dual mode of action starting by depolarizing the motor endplates, but during the blocking process, changing the action to that of a substance competing with ACh. These mutually antagonistic effects result in a rapidly decreasing sensitivity of SOL to C10.

These results demonstrate that a single substance may produce different types of neuromuscular block in the various skeletal muscles of an individual animal. It follows that differences must exist between the neuromuscular junctions of such muscles, but where, in particular, these differences reside remains a matter of speculation.

Other evidence which suggests that different neuromuscular junctions respond differently to similar stimuli are the signs associated with clinical hypocalcaemia in the canine (puerperal tetany) and bovine (parturient paresis). In the early stages of hypocalcaemia, the two species show signs of nervousness and muscular twitching (Nelson, 1960; Resnick, 1964). However, as the hypocalcaemia becomes more acute, the bitch develops signs of tetany and convulsions, whereas the cow becomes paretic, probably usually due to a simultaneous increase in Mg^{++} (Bowen

et al., 1970). In 1963, Voisin suggested that the lowering of plasma $[Ca^{++}]$ in the cow probably caused a relative hypermagnesemia which led to Mg^{++} narcosis and thus paresis.

In 1970, Bowen and his co-workers undertook to study this difference in responses of the cow and the dog to hypocalcaemia. Examination of muscle contractions induced by electrical stimulation of the peroneal nerves of ten cows with hypocalcaemia associated with bovine parturient paresis indicated that two cows had no response before they were given Ca^{++} therapy, six had subnormal responses before therapy, and two had responses which were not affected by therapy. From these results, they inferred that the primary cause of hypocalcaemic paresis was depression of neuromuscular transmission. They further supported this conclusion by recording the depression of hind limb contraction in two cows and observing the reduction in amplitude of the summated motor unit potentials of their peroneus tertius muscle.

Bowen et al. (1970) observed that the suppression of tetany (in two hypocalcaemic, thyroparathyroidectomized dogs), through the use of sub-paralytic doses of dTc, produced signs similar to hypocalcaemic paresis of the cow, with the exception that spontaneous electrical activity of muscles occurred in the dog during drug-induced neuromuscular block but was absent in the cow during hypocalcaemic neuromuscular block. They interpreted this result to mean that a species difference exists in muscle fiber response to hypocalcaemia. The greater sensitivity of calves to dTc as compared with the sensitivity of dogs has been reported by Stowe in 1965. On the basis of species difference in sensitivity to dTc

(Stowe, 1965) and measurement of the margin of safety of neuromuscular transmission in two calves and two dogs (Bowen et al., 1970), the greater sensitivity of neuromuscular transmission in the bovine to hypocalcaemia was attributed to the lower safety margin for transmission present in the bovine; in other words, the degree to which the EPP exceeds firing threshold is less in the bovine than in the canine. Under these conditions, sensitivity to factors reducing EPP amplitude would be greater in the bovine, and this would apply not only to Ca^{++} ions, but also to neuromuscular blocking agents such as dTc.

MATERIALS AND METHODS

The general experimental design has been schematized in Figures 1 and 2. Six groups of animals were used. Animals designated control #1 were studied while their hind limbs had normal blood supply. Animals designated control #2 were studied while one hind limb of each rat was perfused with normal Krebs solution. Animals in the remaining four experimental categories were studied while one hind limb of each animal was perfused with a modification of the Krebs solution (designated modified Krebs #1, #2, #3, and #4). In each experimental category single twitch and tetanic contractions of the EDL and SOL muscles were recorded.

Surgical anesthesia was induced with an intraperitoneal injection of pentobarbital sodium. About 50 mg/kg body wt of the anesthetic was administered initially; this was followed by about one quarter of the initial dose every 1.5 hours. Prior to surgery the animal was pretreated subcutaneously with about 0.6 mg/kg atropine sulphate. Ventilatory pathways were kept free by inserting a piece of 3 mm (internal diameter) tygon[®] tubing in the trachea of the animal. Animals were then placed in dorsal recumbency.

Rectal temperature (T_c) of the animal was maintained at about 37°C throughout the experiment by means of a heating pad placed beneath the animal. The temperature was monitored using a rectal probe attached to a telethermometer (43TD).

In each experiment, either the SOL or the EDL muscle was exposed and dissected to free it maximally from all surrounding tissues, but with

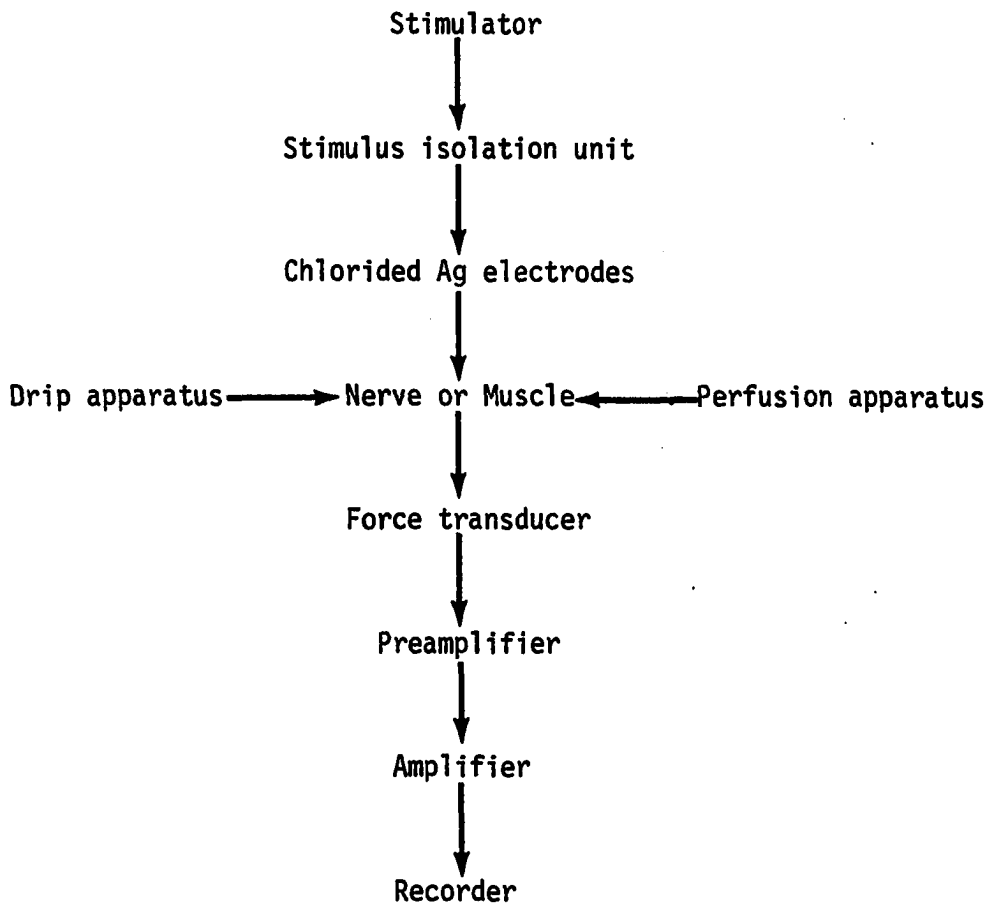


Figure 1. Stimulation and data acquisition processes

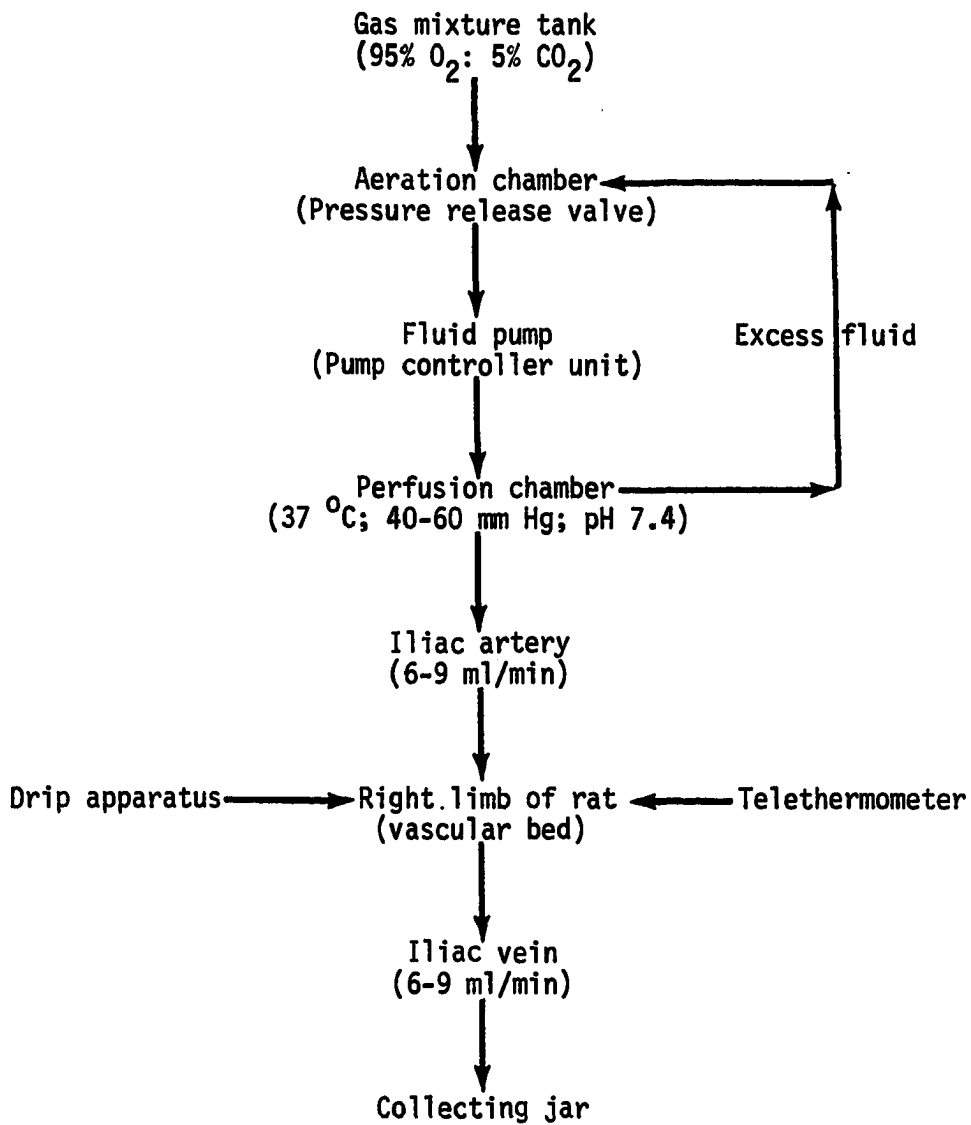


Figure 2. Control sequence of the infusion process

great care to preserve its attachments to both the bone, through its proximal tendons, and the circulatory system (Andrew and Part, 1972). An RF wampler[®] cold cautery scalpel was used throughout surgery to reduce haemorrhage. In addition, a liquid drip was arranged to bathe the muscle preparation continuously with either a normal Krebs (137 mM NaCl, 5 mM KCl, 1 mM MgCl₂, 1 g/l NaHCO₃, 2 g/l glucose, 2 mM CaCl₂) (Table 2b), or a Krebs solution with modified [Ca⁺⁺] and [Mg⁺⁺] (Tables 3b, 4b, 5b, and 6b). A hot plate was used to maintain the temperature of the drip solution (Ts) at approximately 37°C.

Either the SOL muscle nerve (from the tibial nerve) or the common peroneal nerve (which innervates the EDL) was left intact depending on which muscle was being studied in a particular experiment; all other branches of the sciatic nerve to all other muscles in the hind limb were either cut or crushed. The tibia, with the proximal tendon of either the SOL or the EDL still attached to it, was securely clamped (Close, 1964; 1967). The distal tendon of the muscle being studied was cut and connected to a force transducer (Grass FT10C) by means of a stainless steel stylet. The entire experimental set-up was manipulated to ensure a horizontal arrangement of the muscle preparation.

Tensions developed by the muscle were recorded with the isometric force transducer. When in use, the transducer had a total system compliance of about 8×10^{-7} cm/g where compliance or stretchability is a measure of the system's ability to yield to pressure or force without disruption; compliance is defined as the inverse of Young's Modulus, in this case, of the steel stylet used to connect the force transducer to the muscle being

studied. The amplified output from the force transducer was recorded on a polygraph (Grass model 5) pen recorder.

The force transducer was calibrated using gram masses. Grams were then converted to millinewtons (mN) through a multiplication by 9.81 m/sec^2 . The average cross-sectional area of the muscle preparation was estimated as a ratio of the muscle mass (in grams) to the product of the muscle length (in cm) and density (in g/cm^3). The muscle density, determined as 1.13 g/cm^3 , was an approximation from the sum of respective densities of individual components of a muscle cell. Knowing the muscle force of contraction as well as its total surface area, it then became possible to express tension (force per unit area) of a muscle tissue in mN/mm^2 units.

Since the transducer was mounted on a separate micromanipulator it was possible to stretch the muscle without disturbing the set-up of the system. Initially, the muscle was stretched until it just began to develop a passive tension, only then was it caused to contract through nerve stimulation (indirect stimulation); further manipulating the length until a maximal twitch tension was produced indicated that an optimal length had been reached (Buller et al., 1960; Close, 1964). All data were then recorded with the muscle held constant at this optimal length.

The muscle preparation was stimulated (with a Grass S88 stimulator and an SIU5 stimulus isolation unit) indirectly through a pair of chlorided Ag wire electrodes mounted on a micromanipulator to ensure careful positioning on the nerve of the SOL or EDL muscle. Contractions from each muscle preparation were evoked with low (0.1 Hz for SOL and 0.4 Hz

for EDL) and high (400 Hz in either case) frequencies at a fixed duration of 0.4 msec and the maximum tension generated at each frequency recorded. Stimulus voltages were also recorded.

The muscle was also directly stimulated (direct stimulation) by placing the electrodes on the muscle; the presence of similar strength contractions in response to direct and indirect stimulation ensured that all motor units were activated by the indirect stimulation.

In rats of the same species (Wistar), same sex (male), and about the same age and weight (327 g) as those for control #1, the iliac vessels were cannulated for a slow, constant infusion of a normal Krebs solution (control #2) or a modified Krebs solution (modified Krebs #1, #2, #3, and #4). Hypervolemia was effectively eliminated by ligating all major collaterals, particularly, the iliolumbar vessels which drain the limb into the posterior vena cava.

The cannulas used were the intravenous non-radiopaque teflon[®] catheter needle type (20G catheter with 23G inner needle for the artery and 18G catheter with 21G inner needle for the vein). The catheter was carefully inserted in the blood vessel (cannulating the vein before the artery), ligated in place by means of Ethicon[®] nonabsorbable, black braided suture (code A-53), and the needle quickly but carefully withdrawn from the catheter. The arterial cannula was then connected to the perfusing flask (Figure 2) to allow the solution to enter the vascular bed of the hind limb.

At room temperature the Krebs solution has a pH of 7.4; however, after a gas mixture of 95% O₂ and 5% CO₂ has been bubbled through the

solution for at least two hours to raise its pO_2 to a saturated value of not less than 400 mm Hg ($T_s = 37^{\circ}C$), the pH drops to about 7.1. Just before perfusion started, therefore, the pH of the solution was returned to 7.4 by adding a molar solution of NaOH dropwise to it and monitoring its pH with the addition of each drop until the scale of the Corning pH-meter (Corning 7) indicated precisely 7.4. The characteristics of both the influent (Tables 2b-6b) and the effluent (Tables 2c-6c) solutions were determined.

A digital pH/blood gas analyzer 513 (IL 513) was used to measure pH, pCO_2 , and pO_2 . The IL 513 has a measuring range of 6-8 for pH, 0-200 mm Hg for pCO_2 , and 0-2000 mm Hg for pO_2 . It operates over an ambient range of $18-30^{\circ}C$; the sample temperature at set point is $36-38^{\circ}C$. Analysis of 31 tonometered blood samples equilibrated with a gas having a CO_2 tension of 49.5 mm Hg and O_2 tension of 49.5 mm Hg with five IL 513 analyzers over three days yielded repeatabilities of 48.0 ± 0.48 mm Hg and 49.1 ± 0.96 mm Hg for pO_2 and pCO_2 , respectively. A pH study, over five days with one IL 513 analyzer and ten blood samples in the physiological pH range (7.2-7.8) using five different operators, gave a standard deviation for 116 measurements of five milli-pH units.

The basic principle behind the pH electrode involves the development across a sensitive glass membrane of a potential whose magnitude is proportional to the difference in pH of the two solutions separated by this membrane. All glass pH-indicating electrodes have a similar basic design. Contained on one side of a glass membrane is a solution of constant pH. In contact with the other side of this pH-sensitive glass is the solution

of unknown pH. Between the surfaces of the glass membrane, a potential difference develops which is proportional to the pH difference of these solutions. As the pH of the inner solution is constant, this developed potential becomes a measure of the pH of the outer solution.

The direct measurement of $p\text{CO}_2$ using IL- $p\text{CO}_2$ electrodes is an adaptation of a pH measurement. A combined pH-measuring and reference electrode makes contact with a solution behind a gas permeable membrane. CO_2 diffuses across the membrane in either direction in response to a partial pressure difference, equilibrating the inner electrolyte with the external gas pressure. Hydration of CO_2 in the electrolyte water produces carbonic acid causing a change in hydrogen ion activity. The pH electrode senses the change in $[\text{CO}_2]$ as a change in pH of the electrolyte and develops a voltage exponentially related to $p\text{CO}_2$. Thus a ten-fold increase in $p\text{CO}_2$ is nearly equivalent to a decrease in one pH unit.

The IL 513 pH/blood gas analyzer determines $p\text{O}_2$ amperometrically. That is, the $p\text{O}_2$ electrode produces a current, at a constant polarizing voltage (0.6 V), which is directly proportional to the partial pressure of O_2 diffusing to the reactive surface of this electrode. The current is the result of the reduction of O_2 at the cathode.

Production of four electrons accompanies each molecule of O_2 reduced. The $p\text{O}_2$ channel measures this flow of electrons. To make this system specific for O_2 , a polypropylene membrane, permeable to gases but not to contaminants and reducible ions of the sample, covers the electrode.

The serum-calcium-assay method was used to quantitate Ca^{++} , Mg^{++} and P^{3+} in the Krebs solution using the ROTOHEM IIA analyzer (a spec-

trophotometer) and the appropriate corresponding reagent set. For Ca^{++} the Worthington Diagnostics' Ca^{++} Reagent Set (Worthington Diagnostics' catalog #27909) was used. Cresolphthalein complexone in the presence of basic diethylamine reagent reacts with divalent cations to form a red-purple complex absorbing at 550 nm. Specificity for Ca^{++} results from removal of interfering Mg^{++} ions by reacting with 8-hydroxyquinoline. The absorbance of the yellowish calcium-cresolphthalein complexone formed is proportional to the amount of Ca^{++} present. The linearity range of the response of the instrument to Ca^{++} is from 0 to 18 mg/dl.

For Mg^{++} the working reagent is called Mg^{++} Rapid Stat Kit (Worthington Diagnostics' catalog #45500). The reagent kit contains calmagite, which is bound to a mixture of the 9-ethyleneoxide adduct of p-nonylphenol and polyvinylpyrrolidone. These latter materials prevent interference by proteins which would otherwise alter the spectrum of calmagite. Potassium hydroxide keeps the calmagite as the blue alkaline ionic species. The addition of Mg^{++} salts causes the formation of the red Mg^{++} complex of calmagite which absorbs at 532 nm. Ca^{++} interference is eliminated by preferential combination with EDTA which is present in the system in the form of a salt. Interference by heavy metals is prevented by the presence of cyanide. The linear range is from 1.2 to 7.3 meq/l. Thus in MK #3 and MK #4, the ROTOCHEM IIA was not capable of detecting the level of Mg^{++} in the Krebs solution since $[\text{Mg}^{++}]_e$ in both MK #3 and MK #4 was below 1.2 meq/l. Since 1 mM MgCl_2 in CT #2 and MK #1 yielded an average $[\text{Mg}^{++}]_e$ of about 2.0 meq/l (Tables 2b and 3b) and 2 mM MgCl_2 in MK #2 (Tables 3b and 4b) an average of 4.0 meq/l, the $[\text{Mg}^{++}]_e$ in 0.1 mM MgCl_2

used for MK #3 and MK #4 was calculated to be 0.2 meq/l.

P^{3+} is quantitated by means of a Worthington Inorganic Phosphorus Reagent Set (Worthington Diagnostics' catalog #27319). The technique of determination involves the photometric measurement of the blue phosphomolybdate complex which forms when the sulphuric acid and the ammonium molybdate content of the reagent come into contact with inorganic phosphorus. This is done under conditions which do not allow excess molybdate to be reduced. The increase in formation of the unreduced phosphomolybdate complex measured at 340 nm is directly proportional to the amount of inorganic P^{3+} present. The linearity response ranges from 0 to 20 mg/dl.

The repeatability of the ROTOCHEM IIA procedures was determined by analyzing 80 human patient serum and plasma specimens which were also analyzed by the established atomic absorption method. By comparison, a student $t = 1.23$ (which was insignificant) was obtained.

Na^+ and K^+ were measured with the IL 343 Flame Photometer. The sample is thoroughly mixed with air and fuel, and forced into a burner flame. The combustion of propane provides sufficient energy to break apart molecules or complex ions into neutral atoms and to excite the alkali atoms to emit a characteristic set of wavelengths. Light from the flame passes through a long upper clear window of a glass chimney, through three separate filters and onto three photodetectors. Each filter has a fixed narrow bandpass centered on the characteristic wavelength of Na^{++} (589 nm), Li^+ (671 nm) or K^+ (766 nm). The phototube behind each filter produces a current output which is directly proportional to the intensity of the

light striking it, that is, to the intensity of the emission of Na^+ , K^+ or Li^+ .

Random changes in flame temperature and various chemical interferences can cause fluctuations in the emission signal, rendering it fairly unstable. To compensate for this inherent instability in the output, Li^+ is added in a constant amount to both samples and functions as an internal standard. The IL 343 electronically compares the signal from the variable $[\text{Na}^+]$ or $[\text{K}^+]$ in the sample to the signal from the constant $[\text{Li}^+]$ and reports the ratio of these two quantities directly in units of concentration of the analyzed element. Random fluctuations in the flame thus affect both internal standard and Na^+ or K^+ alike; and the ratio remains unaffected, and a stable, accurate readout is obtained. The linear readout range is 0 to 250 meq/l for both Na^+ and K^+ with repeatabilities being ± 0.5 meq/l for Na^+ and ± 0.02 meq/l for K^+ .

Cl^- was determined coulometrically using the Corning Model 920M Chloride Meter. The operation of the 920M is based upon the established principle of titration of Cl^- with Ag^+ ions generated coulometrically from an Ag^+ anode. A constant dc-voltage applied across a pair of Ag^+ electrodes immersed in the diluted sample causes release of Ag^+ ions into the mixture. The Ag^+ ions combine with the Cl^- ions present in the sample and precipitate as AgCl . When all the Cl^- has reacted, the $[\text{Ag}^+]$ increases, causing the conductivity of the mixture to rise. Sensing electrodes detect this rise in conductance and stop the titration. Since titration of Cl^- ion is at a constant rate, the instrument calculates Cl^- levels directly from elapsed titration time. Results are displayed in units of meq/l of

Cl^- within a linearity range of 20 to 350 meq/l and a repeatability of ± 1.5 meq/l for every 25 Cl^- determinations.

Samples to be analyzed for pH, pCO_2 , pO_2 , Ca^{++} , Mg^{++} , P^{3+} , Na^+ , K^+ , and Cl^- were taken within the interval between start of occlusion and end of 20 min of perfusion, stored in a refrigerator, and analyzed a day or two later. Samples for pH, pO_2 and pCO_2 analyses were kept as air-tight as possible (using rubber corks) to minimize equilibration between the Krebs and atmospheric gases.

Figure 2 is a block diagram illustrating the control of the infusion process. The total pressure in the system was provided by the bubbling of the gas mixture through the Krebs solution. An increase or decrease in perfusion pressure (40-60 mm Hg) was thus almost completely dependent on the rate of aeration as well as the rate at which the aerating gas mixture was allowed to escape from the aeration chamber via the pressure release valve. But once established, the perfusion pressure was maintained constant by means of a pump-controller unit (Masterflex® model WZIRO31) which constantly replaced the output from a perfusion flask with an equal volume per unit time from the aeration flask. The optimum flowrates (6-9 ml/min) at both the iliac artery (inflow) and the iliac vein (effluent) were measured by means of a stop watch. A feedback connection from the perfusion flask to the aeration flask ensured that any excess fluid found its way back into the system and thereby allowed only about 6 ml/min of Krebs to supply the vascular bed of the muscle being studied.

Direct and indirect muscle stimulation parameters and tension

development were monitored in animals perfused with normal Krebs solution and compared to those from the intact control animals. Since the results were similar, several additional experiments in which modified Krebs (MK) solutions were infused were performed. The modifications were:

1. Decreased $[Ca^{++}]$ and normal $[Mg^{++}]$ (Table 3b) or MK #1
2. Decreased $[Ca^{++}]$ and increased $[Mg^{++}]$ (Table 4b) or MK #2
3. Normal $[Ca^{++}]$ and decreased $[Mg^{++}]$ (Table 5b) or MK #3
4. Decreased $[Ca^{++}]$ and decreased $[Mg^{++}]$ (Table 6b) or MK #4

By comparing the responses to direct and indirect stimulation in the experiments using a modified Krebs solution to those in the experiments using normal Krebs, it was possible to determine whether changes in tension seen with altered $[Ca^{++}]_e$ and $[Mg^{++}]_e$ were due to transmission changes or muscle excitability and contractility changes. Consistent changes in indirect stimulus voltage would indicate an effect on nerve excitability.

The one-way analysis of variance was used to test if observed differences between any two and among all sample means could be attributed to chance (null hypothesis) or whether they were indicative of actual differences between and among the corresponding population means. The confidence level used was 0.05.

In an additional set of experiments 0.5 mg/l of insulin (24 units/mg) was added to the Krebs solution and all the experimental categories above were repeated to determine how useful insulin, as a facilitator of glucose entry into muscle cells, would have been as a component of the Krebs solution used in the major experiments. The number of rats in each experimental category was 2. Statistical analyses were as already discussed.

RESULTS AND DISCUSSIONS

Perfusion Techniques

Figure 2 illustrates the control sequence in perfusing the EDL or SOL muscle. The flowrate of 6 ml/min (Table 10) seemed optimal (for most of the cases) in sustaining the right hind limb throughout the period of recording and in preventing the animal from dying as a result of hyper- or hypovolemia. There were isolated cases that required up to 9 ml/min as the optimal flowrate. As a whole, differences among the samples are attributable to chance. Darrah (1982) reports of a calculated value of 7-8 ml/min which lies within our experimentally estimated range of 6-9 ml/min.

The driving pressure of perfusion in the set-up of the system varied from one animal to another, ranging from 40 to 60 mm Hg at any established optimal rate of flow through the vascular bed of the Wistar hind limb (Table 10). Such differences in perfusion pressure among the rats could be attributed to three probable factors. First, the vascular bed resistance could be specific to each rat irrespective of sameness of breed; it is highly unlikely that all animals of any particular breed will possess the same number of capillaries per hind limb vascular bed. During the exploratory stages in the perfusing techniques, Sprague-Dawley rats (instead of Wistar) were used, and the perfusion pressures were observed to range from 34 to 48 mm Hg, indicating that Sprague-Dawley rats probably have (on the average) lower vascular bed resistance than Wistar. Second,

both Ca^{++} and Mg^{++} are known to affect the resistance of the vascular bed (Stainsby, 1973). It is possible that the gravity of such an effect could be unique to each animal. Furthermore, in solutions like MK #2 (decreased Ca^{++} and increased Mg^{++}) the vasodilating effect from both Ca^{++} and Mg^{++} on the smooth muscle of the blood vessels did actually synergise to cause the greatest decrease in resistance to flow observed throughout the period of experimentation (Table 10). Generally, pressure values were lower than the average of 50 mm Hg when MK #1 (decreased Ca^{++}) and MK #2 were being perfused, with MK #2 values averaging the lower of the two sets. Since MK #3 contained low Mg^{++} its vasoconstricting effect resulted in perfusion pressures that were generally higher than the average. MK #4 contained both low Ca^{++} (vasodilating effect) and low Mg^{++} (vasoconstricting effect). Thus, the two effects offset each other and yielded perfusion pressure values that seemed clustered around the average. The means of the pressure values for all categories of perfusion in Table 10 (except between CT #2 and MK #4) were significantly different. Third, the critical interval (T10) between the moment the iliac vessels were occluded to allow cannulation and the time the perfusion was started is likely to have had some effect on the individual perfusion pressures observed. Typically, the interval varied between 5 and 10 min. This could have resulted in different perfusion pressures since different time delays could cause different degrees of blood clots in the blood vessels. A T10 beyond 10 min increased the likelihood of the experiment being terminated as a result of excessive blood clots which would maximally resist the perfusion of the capillaries. Any attempt to force the liquid through the blood clot by generating

excessive pressure in the perfusion system caused either the cannulated blood vessel to rupture or one of the two flasks in the perfusion equipment (Figure 2) to explode.

Another serious threat in exceeding T10 is hypoxia to which the nerve reacts more dramatically than the muscle. In preliminary control #2 experiments such instances did occur; indirect stimulation yielded a remarkably more diminished twitch amplitude with abnormally longer duration per impulse than was observed with direct stimulation, a trend that deteriorated rather rapidly to near zero in a few minutes. Since indirect stimulation always preceded the direct, a decreased and prolonged indirect response could not be attributed to a sequential delay in stimulation; hypoxia seemed more likely to be the cause.

Hypoxia-induced results (decreased tension and increased duration) also occur (observed in preliminary experiments) when the pO_2 of the solution being perfused happens to be below about 250 mm Hg. In these experiments, the critical value of pO_2 at which hypoxic effects can occur was not determined, and therefore, it might be erroneous for a researcher to assume that a pO_2 value just above 250 mm Hg will be safe to use. A safe value may be considered as equal to or greater than 400 mm Hg (Table 9).

The characteristics of the Krebs solution used to perfuse the hind limbs of the animals have been shown in Tables 2b-6b and Tables 2c-6c. Tables 7b and 8b show the average changes in ionic concentrations that occurred during perfusion of EDL and SOL respectively. Sample values for pH, pCO_2 and pO_2 have also been tabulated (together with their means and standard deviations) in Table 9. The mean pO_2 difference was found to be

370.9 mm Hg. Using 0.003 ml O_2 /dl blood/mm Hg pO_2 (Ganong, 1977b), optimum perfusion rate of 6 ml/min, and an average rt-hind-limb-wt of 24 g, the amount of O_2 consumed was calculated to 2.78 ml O_2 /kg/min. Ganong (1977a) indicates that skeletal muscle uses 2.0 ml O_2 /kg/min; the higher calculated value of O_2 usage is reasonable considering the fact that the right hind limb includes not only muscle mass but also bones, blood vessels, nerves, and skin, all of which contributed to the higher O_2 consumption.

The significant decrease in pH (Table 9) from 7.27 to 7.09 pH-units correlates with the significant increase in the CO_2 content of the perfused Krebs from 52.0 to 88.7 mm Hg; the pCO_2 increase which occurred between influent and effluent solutions accounts for the increase in the acidity of the solution as evidenced by the corresponding decrease in pH-units. At the time of perfusion the influent pH was kept at 7.4 as far as the pH-meter (Corning 7) could indicate. However, the IL 534 pH/blood gas analyzer consistently gave lower influent readings (Table 9) probably due to the storage of the sample prior to the analysis.

$[Cl^-]$ showed a net significant decrease between influent and effluent in all experiments that involved perfusion, the only exception being SOL MK #2. Changes in $[Mg^{++}]$ and $[Na^+]$ were not significant in all experimental types except EDL MK #2 for $[Na^+]$. For $[Ca^{++}]$ the significant changes were EDL MK #4, SOL MK #1, SOL MK #2, and SOL MK #4. Statistically, $[P^{3+}]$ changes in all experimental categories where Krebs was perfused were not attributable to chance. In SOL MK #1 and EDL MK #1, the changes in $[K^+]$ during Krebs perfusion were statistically insignificant; all other $[K^+]$ changes in the remaining experimental categories were found significant.

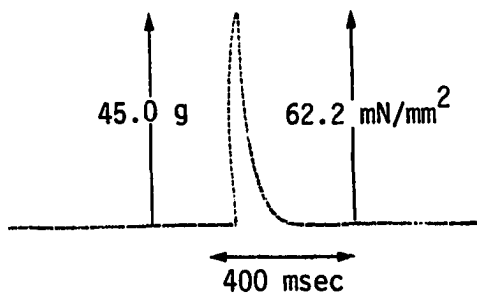
The significant decrease in Cl^- level and the increase (significant or otherwise) in the remaining ionic levels, especially in $[P^{3+}]$, seem to suggest that the Krebs solution was not perfectly balanced in its specific ionic compositions. Thus the Krebs either gained (+) or lost (-) something as it progressed through the vascular bed. While some of these changes were significant, they did not seem to follow a specific trend to enable any inference to be drawn as to whether changes were greater or less in modified or normal Krebs solution.

Control Data #1: Intact Animal

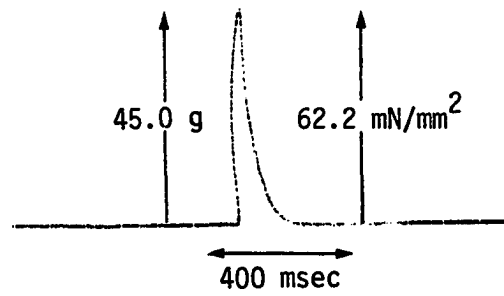
Figure 3 displays sample tracings from muscles with intact vascular systems to indicate that the indirect and direct stimulus voltages caused all motor units of either EDL or SOL to fire. This judgement was based on the similarity in amplitudes of tension elicited both through nerve stimulation (indirect stimulation) and through muscle stimulation (direct stimulation). Values obtained as control data from the intact animal (CT #1) for both EDL and SOL neuromuscular systems have been shown in Table 1; the mean values are in Tables 7a (for EDL at 0.4 pps) and 8a (SOL at 0.1 pps). In SOL both indirect and direct stimulations yielded 35.0 mN/mm^2 , but in EDL there occurred a slight insignificant difference between indirect (62.2 mN/mm^2) and direct (61.1 mN/mm^2) values caused by the death of rat #5 just before direct recording was started.

The choice of 0.1 pps and 0.4 pps as frequencies of stimulation for SOL and EDL respectively stemmed from the findings by Eccles et al.,

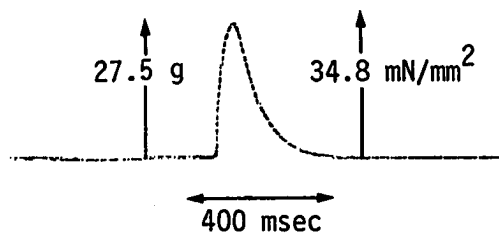
a) Indirect EDL stimulation



b) Direct EDL stimulation



c) Indirect SOL stimulation



d) Direct SOL stimulation

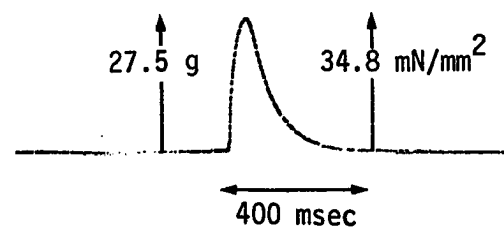


Figure 3. Sample tracings from muscles with intact vascular bed

Table 1. Data from muscles with intact vascular system ($T_c = 37^{\circ}\text{C}$)

Rat #	Rat wt (g)	Muscle			Tension			
		type	wt (mg)	length (mm)	Indirect stim		Direct stim	
					(g)	(mN/mm^2)	(g)	(mN/mm^2)
1	333	EDL	228.8	27	48.0	62.8	48.0	62.8
2	334	EDL	227.9	26	49.5	62.6	49.5	62.6
3	330	EDL	202.7	27	42.0	62.0	42.0	62.0
4	330	EDL	224.7	28	45.0	62.2	45.0	62.2
5	331	EDL	204.4	28	40.5	61.5	36.8 ^a	55.9 ^a
6	319	SOL	188.5	23	25.5	34.5	25.5	34.5
7	323	SOL	235.7	23	33.0	35.7	33.0	35.7
8	323	SOL	208.3	24	27.8	35.5	27.8	35.5
9	328	SOL	195.0	23	26.3	34.4	26.3	34.4
10	332	SOL	188.5	24	24.8	35.0	24.8	35.0

^a Animal died just before direct recording was done.

(1958) that the natural physiological discharge frequencies are approximately 10 Hz (for SOL) and 40 Hz (for EDL). These findings have also been used by Gertler and Robbins (1978) to study differences in neuromuscular transmission in red and white muscles. Since 0.1 and 0.4 have the same proportionality as 10 and 40, the basis of isometric twitch comparison at those two frequencies for the two muscles was deemed fair.

Tensions have been presented in both gram (g) and millinewton per millimeter squared (mN/mm^2) to show that the usual expression of tension values in g alone can sometimes be misleading unless it is pointed out (through mN/mm^2) that the force per unit area or tension may or may not have changed much despite apparent differences in amplitudes for any set of similar muscle types being compared. Table 1 is a good illustration of this point in which tension values in g show a greater degree of variability than those in mN/mm^2 .

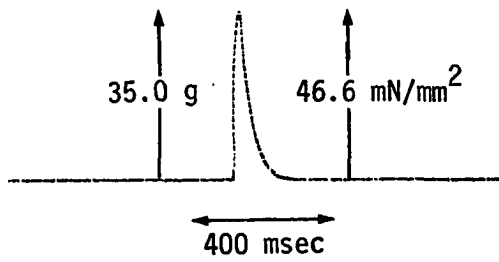
The mean tension of 45.0 g or 62.2 mN/mm² for EDL (Table 7a) was found to be quite close to Close's (1964, 1967) single EDL twitch presentation of 44.57 g. The mean value for SOL was 27.5 g or 35.0 mN/mm² (Table 8a) and this was also quite comparable to Close's (1964; 1967) single SOL twitch of about 26 g (deduced from calibration).

Control Data #2: Normal Krebs Perfusion

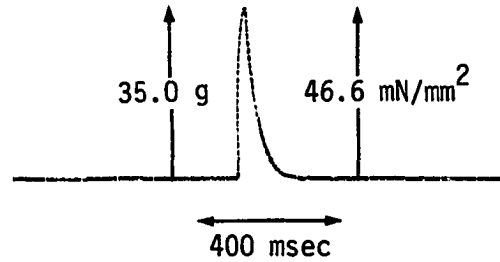
The ionic characteristics of the control Krebs (CT #2) have been tabulated in Table 2b, and Figure 4 shows sample recordings from muscles perfused with this solution. Again, there is a sameness of indirectly and directly stimulated muscle twitches to indicate that all motor units were firing. Individual tension values for both EDL and SOL are shown in Table 2a; means as well as standard deviations for EDL and SOL are shown in Tables 7a and 8a, respectively.

For EDL the average tension was found to be 35.0 g or 46.6 mN/mm²; for the SOL the value was 21.6 g or 26.0 mN/mm². Compared with CT #1, the EDL and SOL tensions in CT #2 depreciated by about 25.1% and 25.7%, respectively; these changes were not surprising considering the difficulties of perfusing an entire vascular bed with an artificial solution. It was expected that with about 75% of the tension recorded in intact animals occurring in animals perfused with normal Krebs, any changes due to the subsequent ionic modifications in the solution should be conspicuous enough to serve the purpose of proving or disproving the hypothesis.

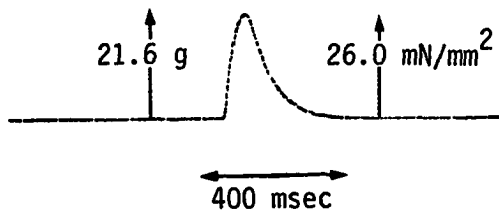
a) Indirect EDL stimulation



b) Direct EDL stimulation



c) Indirect SOL stimulation



d) Direct SOL stimulation

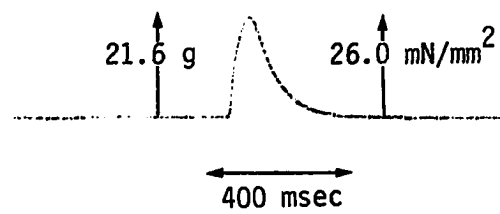


Figure 4. Sample tracings from muscles perfused with normal Krebs

Table 2a. Data from muscles perfused with normal Krebs ($T_c = 37^{\circ}\text{C}$)

Rat		Muscle			Tension			
#	wt	type	wt	length	Indirect stim		Direct stim	
	(g)		(mg)	(mm)	(g)	(mN/mm ²)	(g)	(mN/mm ²)
11	324	EDL	223.6	26	36.0	46.4	36.0	46.4
12	325	EDL	234.4	26	38.3	47.1	38.3	47.1
13	325	EDL	201.9	27	31.5	46.7	31.5	46.7
14	322	EDL	217.4	25	36.0	45.9	36.0	45.9
15	327	EDL	211.5	27	33.0	46.7	33.0	46.7
16	331	SOL	223.9	24	21.8	25.9	21.8	25.9
17	330	SOL	201.4	23	20.3	25.7	20.3	25.7
18	332	SOL	209.4	22	22.5	26.2	22.5	26.2
19	327	SOL	220.6	23	22.5	26.0	22.5	26.0
20	321	SOL	205.9	23	21.0	26.0	21.0	26.0

Table 2b. Ionic levels of the influent normal Krebs ($T_s = 37^{\circ}\text{C}$)

Rat	[Ca ⁺⁺]	[Mg ⁺⁺]	[P ³⁺]	[Na ⁺]	[K ⁺]	[Cl ⁻]
#	(mg/dl)	(meq/l)	(mg/dl)	(meq/l)	(meq/l)	(meq/l)
11	7.7	2.0	3.1	163	5.1	150
12	7.7	2.0	3.0	163	5.0	149
13	7.7	2.0	3.0	161	5.0	150
14	7.6	2.0	3.0	163	5.0	150
15	7.7	2.0	3.0	162	5.0	150
16	7.7	2.1	3.0	163	5.0	150
17	7.8	2.0	3.0	163	5.0	150
18	7.6	2.1	3.1	162	5.1	149
19	7.7	2.1	3.1	162	5.0	149
20	7.7	2.0	3.0	163	5.1	151

Table 2c. Ionic levels of the effluent normal Krebs

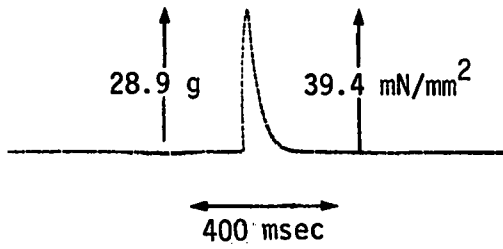
Rat	[Ca ⁺⁺]	[Mg ⁺⁺]	[P ³⁺]	[Na ⁺]	[K ⁺]	[Cl ⁻]
#	(mg/dl)	(meq/l)	(mg/dl)	(meq/l)	(meq/l)	(meq/l)
11	7.7	2.1	4.3	159	5.5	144
12	7.8	2.1	4.4	162	5.7	147
13	7.8	2.2	4.4	166	5.9	146
14	7.8	2.1	4.4	166	5.8	146
15	7.7	2.1	4.4	164	5.8	147
16	7.7	2.0	4.4	163	5.6	146
17	7.8	2.0	4.3	163	5.6	146
18	7.6	2.0	4.3	166	5.8	146
19	7.8	2.1	4.3	165	5.8	147
20	7.7	2.1	4.4	160	5.8	145

Modified Krebs #1: Decreased $[Ca^{++}]$ and Normal $[Mg^{++}]$

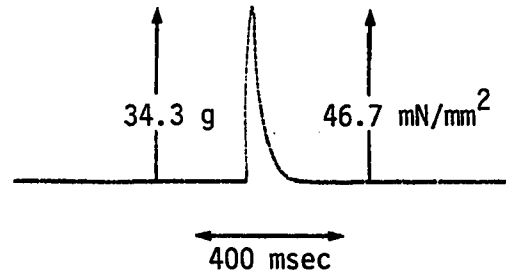
Figure 5 shows the effect of decreasing $[Ca^{++}]$ from 7.7 to 4.8 mg/dl (Table 3b) on the isometric twitches of both EDL and SOL. As discussed earlier Ca^{++} is required for induction of ACh release. Lack of Ca^{++} results in no EPP generation although the AP due to the motor nerve stimulation still invades the nerve terminal (Rahamimoff, 1976). Thus a decrease in Ca^{++} should result in a proportionate decrease in capacity to activate transmitter release. The resulting decrease in ACh release should cause a correspondingly limited number of NMJs to produce supra-threshold EPPs, leading to fewer MAPs which would ultimately cause fewer muscle cells to contract. Consequently, the observed indirect stimulation twitches (Figures 5a and 5c) show statistically significant depreciation. This decrease cannot be attributed to degeneration of the NMS since the indirect stimulation always preceded the direct.

In contrast, isometric twitches in Figures 5b and 5d (direct stimulation) exhibit higher amplitudes than those in Figures 5a and 5c (indirect stimulation). Transmitter release is not involved during direct stimulation and therefore Ca^{++} insufficiency is no longer the critical factor in determining the number of fibers or motor units that respond to a stimulus. Table 3a shows tension values obtained from muscles perfused with modified Krebs #1 using indirect and direct stimulation techniques. The average EDL indirect tension measured in MK #1 (in mN/mm^2) showed a percentage decrease of 15.5% as compared to CT #2 whereas the percentage decrease for SOL turned out to be 41.9%, indicating that SOL NMJ

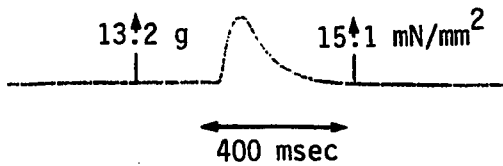
a) Indirect EDL stimulation



b) Direct EDL stimulation



c) Indirect SOL stimulation



d) Direct SOL stimulation

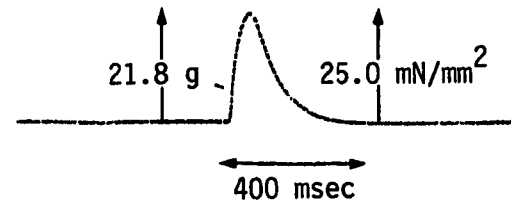


Figure 5. Sample tracings from muscles perfused with modified Krebs #1

Table 3a. Data from muscles perfused with modified Krebs #1 ($T_c = 37^{\circ}\text{C}$)

Rat		Muscles			Tension			
#	wt	type	wt	length	Indirect stim		Direct stim	
	(g)		(mg)	(mm)	(g)	(mN/mm ²)	(g)	(mN/mm ²)
21	327	EDL	181.8	26	26.3	41.7	29.3	46.5
22	324	EDL	228.0	26	28.5	36.0	36.0	45.5
23	326	EDL	222.8	27	30.0	40.3	34.5	46.3
24	328	EDL	212.2	26	29.3	39.8	36.0	48.9
25	328	EDL	230.3	27	30.3	39.4	35.7	46.4
26	335	SOL	227.3	24	13.5	15.8	22.5	26.3
27	324	SOL	222.1	23	13.5	15.5	23.3	26.7
28	338	SOL	234.6	23	15.0	16.3	21.0	22.8
29	335	SOL	218.5	23	12.0	14.0	19.5	22.8
30	328	SOL	218.5	23	12.0	14.0	22.5	26.3

Table 3b. Ionic levels of the influent modified Krebs #1 ($T_s = 37^{\circ}\text{C}$)

Rat	[Ca ⁺⁺]	[Mg ⁺⁺]	[P ³⁺]	[Na ⁺]	[K ⁺]	[Cl ⁻]
#	(mg/dl)	(meq/l)	(mg/dl)	(meq/l)	(meq/l)	(meq/l)
21	4.9	1.8	3.2	162	5.0	155
22	4.9	1.8	3.2	162	5.0	156
23	4.8	1.9	3.1	160	5.0	152
24	4.9	1.9	3.1	161	5.0	154
25	4.8	1.9	3.0	160	5.0	154
26	4.8	2.0	3.0	166	5.1	150
27	4.3	2.0	2.8	164	5.0	150
28	4.4	1.9	2.9	161	5.0	151
29	4.4	1.9	2.8	161	5.0	151
30	4.7	2.0	3.1	161	5.2	148

Table 3c. Ionic levels of the effluent modified Krebs #1

Rat	[Ca ⁺⁺]	[Mg ⁺⁺]	[P ³⁺]	[Na ⁺]	[K ⁺]	[Cl ⁻]
#	(mg/dl)	(meq/l)	(mg/dl)	(meq/l)	(meq/l)	(meq/l)
21	5.0	1.9	3.7	158	5.2	147
22	5.0	1.9	3.6	160	5.3	145
23	5.0	1.9	3.6	159	5.3	146
24	5.0	1.9	3.6	159	5.3	145
25	4.9	1.9	3.6	159	5.2	145
26	5.1	2.2	4.4	158	5.2	146
27	5.0	1.9	4.5	157	5.3	146
28	5.1	2.0	3.9	166	5.5	146
29	5.1	2.0	3.9	167	5.6	150
30	5.1	2.0	3.9	167	4.9	144

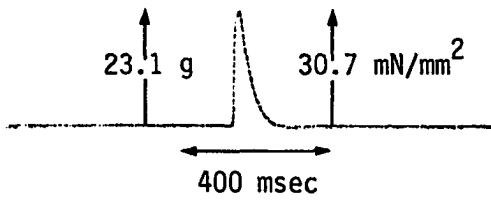
responds more drastically to a decrease in $[Ca^{++}]$ than the EDL NMJ. Statistically, no significant differences were detected from either EDL or SOL tension values produced through direct stimulation when MK #1 values (Table 3a) were compared with normal Krebs values (Table 2a). Tables 7a (EDL) and 8a (SOL) are further confirmations of insignificant differences between the direct tension values of muscles perfused with MK #1 and those with normal Krebs.

It was thought necessary to compare only recordings that were done at the same recording period (T30) from start of perfusion for 20 min, but never greater than 30 min from occlusion. Preliminary experimentation had shown that after T30 the amplitude seemed to be steadily declining with respect to time. This steady decline in amplitude, which was not observed with normal Krebs perfusion beyond T30, may be attributable, in part, to the fact that the decrease in $[Ca^{++}]_e$ in MK #1 may have resulted in a disturbance of the equilibrium that should exist between $[Ca^{++}]_e$ and $[Ca^{++}]_i$ for normal or full contractile processes to occur. Subsequently, a shift in Ca^{++} equilibrium from inside to outside manifested itself as a decrease in amplitude of tension elicited through direct stimulation.

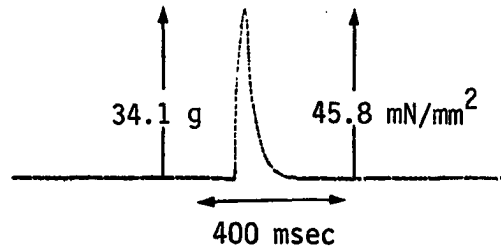
Modified Krebs #2: Decreased $[Ca^{++}]$ and Increased $[Mg^{++}]$

Table 4b shows the characteristics of the modified Krebs #2 (MK #2) used to perfuse both the EDL and the SOL neuromuscular systems. The Ca^{++} level was again reduced from 7.7 to 4.8 mg/dl; in addition, the Mg^{++} level was raised from 2.1 to 4.1 meq/l.

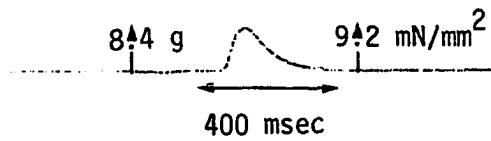
a) Indirect EDL stimulation



b) Direct EDL stimulation



c) Indirect SOL stimulation



d) Direct SOL stimulation

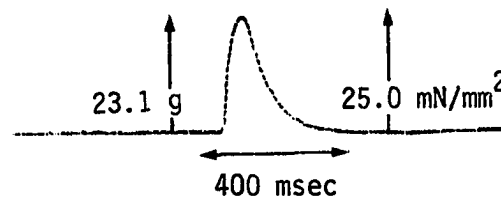


Figure 6. Sample tracings from muscles perfused with modified Krebs #2

Table 4a. Data from muscles perfused with modified Krebs #2 ($T_c = 37^{\circ}\text{C}$)

Rat		Muscle			Tension			
#	wt	type	wt	length	Indirect stim		Direct stim	
	(g)		(mg)	(mm)	(g)	(mN/mm ²)	(g)	(mN/mm ²)
31	330	EDL	226.8	26	25.5	32.4	36.0	45.7
32	326	EDL	235.8	26	27.0	33.0	35.3	43.1
33	326	EDL	177.9	26	18.7	30.3	36.0	58.3
34	325	EDL	237.0	25	24.8	29.0	36.0	42.1
35	329	EDL	187.1	25	19.5	28.9	27.0	40.0
36	324	SOL	225.1	22	6.8	7.3	24.0	26.0
37	334	SOL	230.0	22	8.3	8.8	24.0	25.4
38	322	SOL	235.3	23	6.0	6.5	21.0	22.8
39	338	SOL	214.9	23	7.5	8.9	24.0	28.5
40	337	SOL	239.0	23	14.3	15.2	22.5	24.0

Table 4b. Ionic levels of the influent modified Krebs #2 ($T_s = 37^{\circ}\text{C}$)

Rat	[Ca ⁺⁺]	[Mg ⁺⁺]	[P ³⁺]	[Na ⁺]	[K ⁺]	[Cl ⁻]
#	(mg/dl)	(meq/l)	(mg/dl)	(meq/l)	(meq/l)	(meq/l)
31	4.9	4.0	2.6	165	4.9	156
32	4.6	4.0	2.6	161	4.9	155
33	4.5	4.1	2.4	165	4.9	156
34	4.5	4.1	2.5	165	4.9	158
35	4.4	4.2	2.7	166	4.9	156
36	4.9	4.1	3.1	166	5.1	152
37	4.4	4.1	3.1	162	5.1	150
38	4.7	4.1	2.8	158	5.0	150
39	4.6	4.1	2.7	158	5.2	150
40	4.4	4.0	2.8	166	5.0	151

Table 4c. Ionic levels of the effluent modified Krebs #2

Rat	[Ca ⁺⁺]	[Mg ⁺⁺]	[P ³⁺]	[Na ⁺]	[K ⁺]	[Cl ⁻]
#	(mg/dl)	(meq/l)	(mg/dl)	(meq/l)	(meq/l)	(meq/l)
31	4.8	4.2	3.8	168	5.4	147
32	4.8	4.3	4.0	169	5.4	148
33	4.8	4.1	3.7	168	5.4	149
34	4.7	4.3	3.8	168	5.4	149
35	4.8	4.3	3.6	171	5.5	148
36	5.1	4.0	4.4	162	5.1	144
37	5.0	4.0	4.4	162	5.7	145
38	5.0	3.9	4.3	163	5.7	160
39	5.0	3.9	4.4	163	5.6	147
40	5.1	4.0	4.4	167	5.5	149

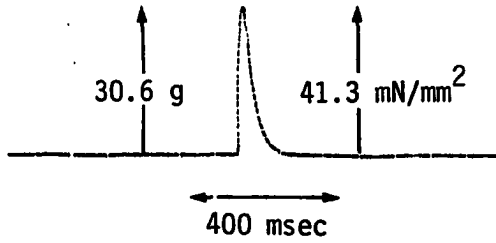
The most critical of increased $[Mg^{++}]$ effects has been described by Jenkinson (1957) and Hubbard (1973) as the inhibition of ACh release. Earlier in this chapter it was discussed that initiation of transmitter release is greatly hindered by decreased levels of Ca^{++} in MK #1. Therefore, increasing $[Mg^{++}]$ and decreasing $[Ca^{++}]$ should be synergistic in blocking ACh release at the NMJ. It seems reasonable then that the recordings in Figure 6 for MK #2 (decreased $[Ca^{++}]_e$, increased $[Mg^{++}]_e$) demonstrate effects that are similar to but more pronounced than those in Figure 5 for MK #1 (decreased $[Ca^{++}]_e$, normal $[Mg^{++}]_e$).

Table 4a shows the values of tension obtained through indirect muscle stimulation when the muscles were perfused with MK #2; Tables 7a (EDL) and 8a (SOL) show the mean values and their standard deviations. While the change (in mN/mm^2) in both EDL and SOL tensions (with respect to CT #2) due to direct stimulation were insignificant, those which resulted from indirect stimulation showed significant depreciations of 34.1% (EDL) and 64.2% (SOL). Thus the effects of decreased $[Ca^{++}]$ and increased $[Mg^{++}]$ yielded more pronounced effects for both EDL and SOL than what the decreased $[Ca^{++}]$ alone (MK #1) produced. Again, the SOL NMJ seemed to be more sensitive of the two types of systems.

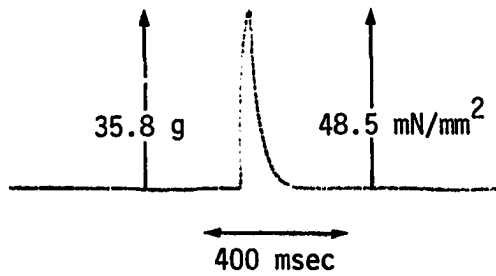
Modified Krebs #3: Decreased $[Mg^{++}]$ and Normal $[Ca^{++}]$

Table 5b shows the characteristics of the influent modified Krebs and Figure 7 is a display of sample recordings from muscles perfused with this solution. The corresponding isometric tensions of EDL and SOL

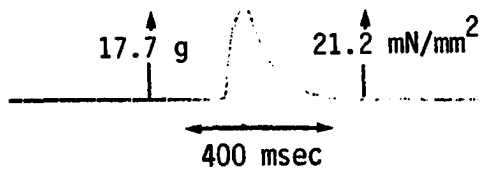
a) Indirect EDL stimulation



b) Direct EDL stimulation



c) Indirect SOL stimulation



d) Direct SOL stimulation

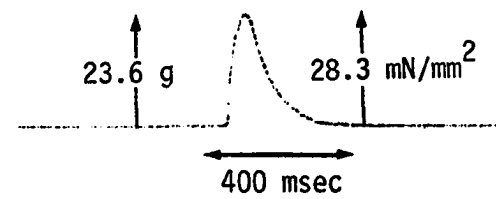


Figure 7. Sample tracings from muscles perfused with modified Krebs #3

Table 5a. Data from muscles perfused with modified Krebs #3 ($T_c = 37^{\circ}\text{C}$)

Rat		Muscle			Tension			
#	wt	type	wt	length	Indirect stim		Direct stim	
	(g)		(mg)	(mm)	(g)	(mN/mm ²)	(g)	(mN/mm ²)
41	329	EDL	212.6	26	31.5	42.7	38.3	51.9
42	322	EDL	221.0	26	28.5	37.2	34.5	45.0
43	316	EDL	172.2	26	27.0	45.2	33.0	55.2
44	322	EDL	220.0	26	33.0	43.2	34.5	45.2
45	340	EDL	249.2	26	33.0	38.2	39.0	45.1
46	324	SOL	220.0	23	15.0	17.4	25.5	29.6
47	320	SOL	200.1	23	16.5	21.0	22.5	28.7
48	332	SOL	238.9	23	21.0	22.4	24.8	26.5
49	318	SOL	205.2	23	18.0	22.4	22.5	28.0
50	317	SOL	201.0	23	18.0	22.8	22.5	28.5

Table 5b. Ionic levels of the influent modified Krebs #3 ($T_s = 37^{\circ}\text{C}$)

Rat #	[Ca ⁺⁺] (mg/dl)	[Mg ⁺⁺] (meq/l)	[P ³⁺] (mg/dl)	[Na ⁺] (meq/l)	[K ⁺] (meq/l)	[Cl ⁻] (meq/l)
41	7.5	***	2.8	164	5.0	149
42	7.6	***	3.1	162	5.0	150
43	7.6	***	3.1	163	4.9	150
44	7.7	***	3.1	163	5.0	151
45	7.5	***	2.8	164	5.0	151
46	7.8	***	2.7	160	5.1	151
47	7.5	***	3.1	160	5.0	151
48	7.5	***	3.1	166	5.0	149
49	7.6	***	3.1	166	4.9	149
50	7.5	***	3.0	160	4.8	148

Table 5c. Ionic levels of the effluent modified Krebs #3

Rat #	[Ca ⁺⁺] (mg/dl)	[Mg ⁺⁺] (meq/l)	[P ³⁺] (mg/dl)	[Na ⁺] (meq/l)	[K ⁺] (meq/l)	[Cl ⁻] (meq/l)
41	7.7	***	4.1	160	5.7	143
42	7.5	***	4.1	160	5.0	144
43	7.8	***	4.4	166	5.0	143
44	7.8	***	4.2	166	5.7	143
45	7.7	***	4.0	166	5.7	142
46	7.7	***	4.4	166	5.3	144
47	7.7	***	4.3	166	5.7	144
48	7.7	***	4.3	162	5.4	147
49	7.5	***	4.3	162	5.5	147
50	7.5	***	4.2	164	5.5	145

***Below the detectable minimum of 1.2 but calculated as 0.2 meq/l.

are tabulated in Table 5a. The mean values are shown in Tables 7a and 8a as 30.6 g or 41.3 mN/mm² for EDL and 17.7 g or 21.2 mN/mm² for SOL. These (values in mN/mm² units) correspond to significant decreases in tension amplitudes of 11.4% (EDL) and 18.5% (SOL) with respect to 46.6 mN/mm² (EDL) and 26.0 mN/mm² of CT #2. Direct tension values did not show any significant changes.

The effect of decreased Mg⁺⁺ from 2.0 to 0.2 meq/l was not expected to be as pronounced as outlined above. The expectation was that the effects of decreased Mg⁺⁺ would not be significantly different from the observations made under control #2, and in fact, seemed to have been established in preliminary experiments in which Mg⁺⁺ was reduced to only about 1.0 meq/l (by calculation from 0.5 mM MgCl₂ used in Krebs).

Jenkinson established in 1957 that the actions of Ca⁺⁺ and Mg⁺⁺ are antagonistic in initiating ACh release but synergistic in decreasing the threshold of excitability. Thus in this instance where [Mg⁺⁺] had been decreased but [Ca⁺⁺] stayed normal some increased neural and muscular excitability as well as some increased ACh release might be expected. Thus a combination of normal Ca⁺⁺ and decreased Mg⁺⁺ should theoretically allow excessive ACh to reach the endplate causing all muscle fibers to twitch. Since all fibers were presumably twitching under direct stimulation, both direct and indirect should have produced the same amplitude of isometric tensions in both EDL and SOL just as was observed under CT #2. Again, this did happen in a preliminary stage but did not repeat itself in the final collection of data. It is possible that the further decrease in [Mg⁺⁺] from 1.0 meq/l to 0.2 meq/l damages the NMJ more

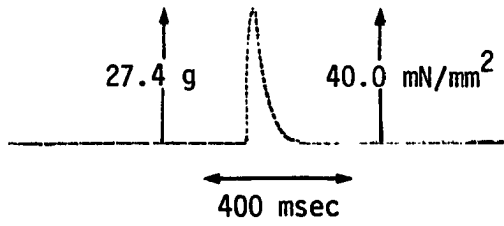
than the muscle causing the tension from indirect stimulation to decrease.

Modified Krebs #4: Decreased $[Mg^{++}]$ and Decreased $[Ca^{++}]$

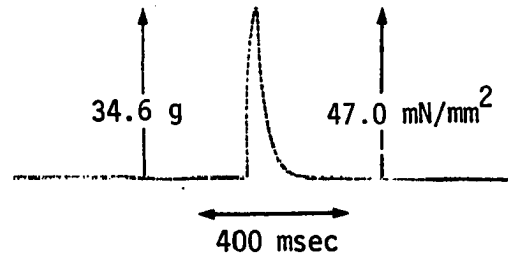
The characteristics of modified Krebs #4 (MK #4) are shown in Table 6b, the isometric tension values of both EDL and SOL in Table 6a, the mean values and their standard deviations in Tables 7a (EDL) and 8a (SOL), and representative sample tracings for muscles perfused with MK #4 in Figure 8. Compared to CT #2, the indirectly stimulated EDL isometric tension (29.3 g or 38.8 mN/mm^2) showed a depreciation of 16.7% while the SOL isometric tension decrease (15.9 g or 20.9 mN/mm^2) valued 19.6% of the CT #2 values. Statistically, the difference between MK #4 and CT #2 indirectly obtained tensions were significant whereas directly obtained tension differences were not. Also, the direct tension values between MK #4 and MK #3 were not significantly different for EDL but were significantly different for SOL for no apparent reason although their corresponding indirect value differences could be attributed to chance.

Like MK #3, these effects of MK #4 were unexpected; however, it may be contended that the increased reduction (compared to CT #2) in EDL tension amplitude from 11.4 (MK #3) to 16.7% (MK #4) as well as that in SOL tension amplitude from 18.5 (MK #3) to 19.6% (MK #4) is attributable to the effect of decreased $[Ca^{++}]$ in MK #4 in addition to the already existing effect of decreased $[Mg^{++}]$ in MK #3. Decreased $[Ca^{++}]$ tends to block ACh release and thereby decrease the EPP, but decreased $[Mg^{++}]$ can partly offset this effect by allowing greater ACh release. Thus the overriding

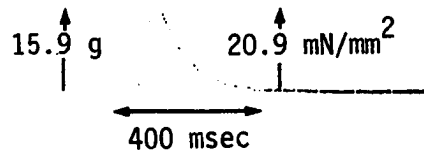
a) Indirect EDL stimulation



b) Direct EDL stimulation



c) Indirect SOL stimulation



d) Direct SOL stimulation

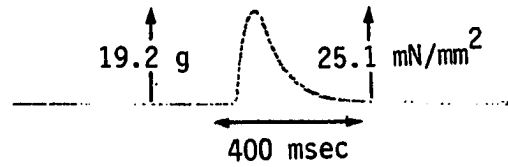


Figure 8. Sample tracings from muscles perfused with modified Krebs #4

Table 6a. Data from muscles perfused with modified Krebs #4 (Tc = 37°C)

Rat		Muscle			Tension			
#	wt	type	wt	length	Indirect stim		Direct stim	
	(g)		(mg)	(mm)	(g)	(mN/mm ²)	(g)	(mN/mm ²)
51	337	EDL	202.5	27	27.0	39.9	34.5	51.0
52	330	EDL	239.5	27	27.8	34.7	35.3	44.1
53	329	EDL	239.9	26	28.5	34.2	36.8	44.2
54	332	EDL	232.8	25	36.0	42.9	42.0	50.0
55	327	EDL	191.0	27	27.0	42.3	36.0	50.4
56	321	SOL	200.0	23	15.0	19.1	16.5	21.0
57	320	SOL	210.0	23	18.0	21.8	21.0	25.5
58	321	SOL	200.3	23	13.5	17.2	21.0	26.7
59	315	SOL	178.4	24	16.5	24.6	18.0	26.8
60	320	SOL	203.3	24	16.5	21.6	19.5	25.5

Table 6b. Ionic levels of the influent modified Krebs #4 (Ts = 37°C)

Rat	[Ca ⁺⁺]	[Mg ⁺⁺]	[P ³⁺]	[Na ⁺]	[K ⁺]	[Cl ⁻]
#	(mg/dl)	(meq/l)	(mg/dl)	(meq/l)	(meq/l)	(meq/l)
51	4.4	***	3.0	163	5.1	150
52	4.5	***	3.0	163	5.0	151
53	4.8	***	3.1	166	5.1	152
54	4.2	***	2.9	160	5.1	160
55	4.4	***	3.1	161	5.1	150
56	4.3	***	3.1	158	5.0	150
57	4.4	***	3.1	157	5.0	151
58	4.7	***	2.7	159	5.0	151
59	4.5	***	2.7	166	5.0	151
60	4.6	***	3.0	166	5.1	151

Table 6c. Ionic levels of the effluent modified Krebs #4

Rat	[Ca ⁺⁺]	[Mg ⁺⁺]	[P ³⁺]	[Na ⁺]	[K ⁺]	[Cl ⁻]
#	(mg/dl)	(meq/l)	(mg/dl)	(meq/l)	(meq/l)	(meq/l)
51	5.0	***	4.2	164	5.6	148
52	4.9	***	4.0	165	5.6	144
53	4.9	***	3.9	165	5.7	143
54	4.9	***	4.4	160	5.4	150
55	5.1	***	4.4	166	5.3	148
56	5.1	***	4.4	159	5.6	150
57	5.0	***	3.8	160	5.6	150
58	5.0	***	3.9	159	5.6	142
59	5.0	***	4.0	167	5.5	143
60	4.9	***	4.4	166	5.0	143

***Below the detectable minimum of 1.2 but calculated as 0.2 meq/l.

Table 7a. Reaction of EDL at 0.4 pps to different calcium and magnesium levels in Krebs solution

Type of Experiment	EDL		Ionic levels		Tension			
	wt (mg)	length (mm)	[Ca ⁺⁺] (mg/dl)	[Mg ⁺⁺] (meq/l)	Indirect stim		Direct stim	
					(g)	(mN/mm ²)	(g)	(mN/mm ²)
CT #1	217.7	27.2	---	---	45.0 ± 3.8	62.2 ± 0.5	44.3 ± 5.1	61.1 ± 2.9
CT #2	217.8	26.2	7.8	2.1	35.0 ± 2.7	46.6 ± 0.4	35.0 ± 2.7	46.6 ± 0.4
MK #1	215.0	26.4	4.9	1.9	28.9 ± 1.6	39.4 ± 2.1	34.3 ± 2.9	46.7 ± 1.3
MK #2	212.9	25.6	4.7	4.0	23.1 ± 3.7	30.7 ± 1.9	34.1 ± 4.0	45.8 ± 2.3
MK #3	215.0	26.0	7.7	***	30.6 ± 2.7	41.3 ± 3.4	35.9 ± 2.6	48.5 ± 4.8
MK #4	221.1	26.5	4.8	***	29.3 ± 3.8	38.8 ± 4.1	36.9 ± 3.0	47.9 ± 3.5

***Below the detectable minimum of 1.2 meq/l but calculated to be 0.2 meq/l.

55

Table 7b. Net ionic gain (+) or loss (-) in Krebs solution during EDL perfusion

Type of Experiment	[Ca ⁺⁺] (mg/dl)	[Mg ⁺⁺] (meq/l)	[P ³⁺] (mg/dl)	[Na ⁺] (meq/l)	[K ⁺] (meq/l)	[Cl ⁻] (meq/l)
Normal Krebs	+0.1	+0.1	+1.4	+1.0	+0.7	-3.8
Modified Krebs #1	+0.1	0.0	+0.5	-2.0	+0.3	-8.6
Modified Krebs #2	+0.2	+0.2	+1.2	+4.4	+0.5	-8.0
Modified Krebs #3	+0.1	----	+1.2	+0.4	+0.4	-7.2
Modified Krebs #4	+0.5	----	+1.2	+1.4	+0.4	-6.0

Table 8a. Reaction of SOL at 0.1 pps to different calcium and magnesium levels in Krebs solution

Type of Experiment	SOL		Ionic levels		Tension			
	wt (mg)	length (mm)	[Ca ⁺⁺]	[Mg ⁺⁺]	Indirect stim		Direct stim	
			(mg/dl)	(meq/l)	(g)	(mN/mm ²)	(g)	(mN/mm ²)
CT #1	203.2	23.4	---	---	27.5 ± 3.3	35.0 ± 0.6	27.5 ± 3.3	35.0 ± 0.6
CT #2	212.5	23.0	7.7	2.1	21.6 ± 1.0	26.0 ± 0.2	21.6 ± 1.0	26.0 ± 0.2
MK #1	224.2	23.2	4.8	2.0	13.2 ± 1.3	15.1 ± 1.1	21.8 ± 1.5	25.0 ± 2.0
MK #2	228.9	22.6	4.8	4.2	8.6 ± 3.3	9.3 ± 3.4	23.1 ± 1.3	25.0 ± 2.2
MK #3	213.1	23.0	7.6	***	17.7 ± 2.2	21.2 ± 2.2	23.6 ± 1.5	28.3 ± 1.1
MK #4	198.4	23.4	4.8	***	15.9 ± 1.7	20.9 ± 2.8	19.2 ± 2.0	25.1 ± 2.4

***Below the detectable minimum of 1.2 meq/l but calculated to be 0.2 meq/l.

56

Table 8b. Net ionic gain (+) or loss (-) in Krebs solution during SOL perfusion

Type of Experiment	[Ca ⁺⁺] (mg/dl)	[Mg ⁺⁺] (meq/l)	[P ³⁺] (mg/dl)	[Na ⁺] (meq/l)	[K ⁺] (meq/l)	[Cl ⁻] (meq/l)
Normal Krebs	0.0	0.0	+1.3	+0.8	+0.7	-3.8
Modified Krebs #1	+0.6	+0.1	+1.2	+0.4	+0.2	-4.0
Modified Krebs #2	+0.4	-0.1	+1.5	+1.4	+0.4	-1.6
Modified Krebs #3	0.0	----	+1.3	+1.6	+0.5	-4.2
Modified Krebs #4	+0.5	----	+1.2	+1.0	+0.4	-5.2

Table 9. Sample values of pH, pCO₂ and pO₂ for the perfused Krebs solution

pH		pCO ₂		pO ₂	
Influent	Effluent	Influent (mm Hg)	Effluent (mm Hg)	Influent (mm Hg)	Effluent (mm Hg)
7.362	7.053	43.6	117.4	601.0	121.4
7.382	7.059	41.3	115.5	582.0	129.4
7.332	7.054	43.4	109.8	563.0	138.4
7.249	7.079	58.4	98.2	608.0	120.2
7.353	7.038	38.2	108.5	563.0	115.4
7.077	7.044	70.2	70.9	426.5	125.4
7.093	7.050	64.5	71.1	410.9	133.4
7.083	7.029	65.9	72.1	425.3	135.8
7.096	7.060	64.1	69.2	414.5	140.8
7.106	7.056	62.3	69.3	407.5	129.4
7.407	7.181	41.9	82.2	531.0	154.6
7.348	7.154	50.3	87.8	534.0	188.5
7.382	7.143	44.2	89.8	539.0	161.8
7.373	7.152	47.0	86.4	533.0	152.5
7.401	7.165	44.4	82.6	541.0	170.1
7.270 _± 0.14	7.088 _± 0.05	52.0 _± 10.9	88.7 _± 17.4	512.0 _± 73.5	141.1 _± 20.6

Table 10. Perfusion pressure values at optimal flowrates of Krebs solution ($T_s = 37^{\circ}\text{C}$)

	Normal Krebs		Modified Krebs #1		Modified Krebs #2		Modified Krebs #3		Modified Krebs #4	
	PP (mm Hg)	FR (ml/min)	PP (mm Hg)	FR (ml/min)	PP (mm Hg)	FR (ml/min)	PP (mm Hg)	FR (ml/min)	PP (mm Hg)	FR (ml/min)
EDL	49	6.0	43	6.0	43	6.2	58	9.0	52	6.0
EDL	40	6.0	43	6.0	40	6.0	60	6.0	48	6.0
EDL	44	6.0	50	7.4	40	6.0	55	6.0	49	6.0
EDL	47	6.0	50	6.6	42	6.4	55	6.0	49	7.0
EDL	50	6.0	40	6.0	41	6.0	57	6.0	52	6.0
SOL	55	6.2	40	6.0	44	6.4	52	6.0	50	8.0
SOL	52	6.2	45	6.0	40	6.0	58	6.6	51	6.0
SOL	60	8.2	40	6.0	40	6.0	60	6.0	52	6.8
SOL	49	6.0	44	6.0	41	6.0	56	6.0	48	6.0
SOL	48	6.0	47	6.2	41	6.0	55	9.0	48	6.0
	49±6	6.2±0.7	44±4	6.2±0.6	41±1	6.1±0.2	57±2	6.7±1.2	50±2	6.4±0.7

effect of MK #4 compared to MK #3 is most likely to be a decreased amplitude in isometric tension due to less transmitter release.

Stimulus Threshold Voltages

The threshold voltages used to stimulate the EDL or the SOL muscle indirectly through the nerve or directly on the muscle were not as expected; it was thought that they would be about the same between controls #1 and #2, and vary among MKs #1, #2, #3, and #4, as well as between the MKs and the controls.

Since the application of current was extracellular, it was expected that between EDL and SOL, the SOL nerve would show the lesser sensitivity by yielding maximum tensions at much higher threshold stimuli than the nerve. The lowest threshold voltages for both systems were expected to be recorded during perfusion with MK #4, SOL NMS threshold being still the higher of the two values. The fact that it did not happen is probably an indication that this method of measuring the thresholds of firing is not sufficiently accurate.

Typical values recorded for single isometric twitches clustered around 45 V (EDL, direct stim), 7 V (EDL, indirect stim), 50 V (SOL, direct stim), and 10 V (SOL, indirect stim). Deviations from the above values were insignificant.

Tetanic Contractions

Figures 9-14 are sample tracings of tetanic contractions from EDL in all six experimental phases (CT #1 to MK #4); corresponding recordings for SOL are shown as Figures 15-20.

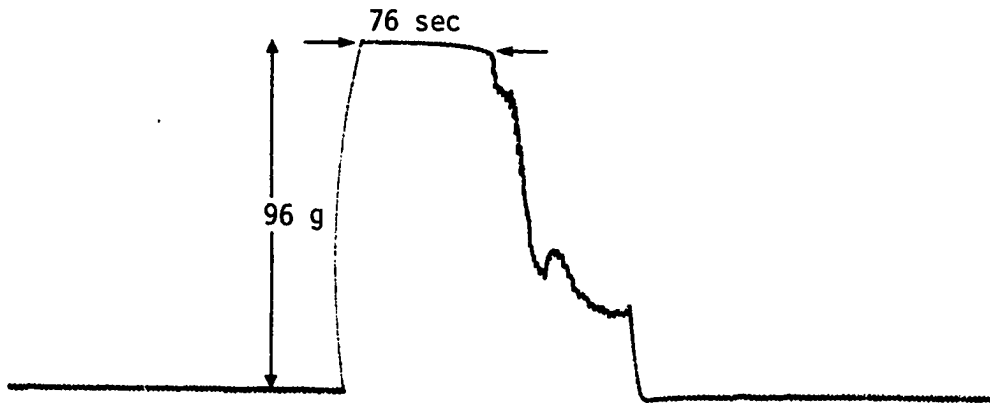
The greatest setback in the tetanic recordings was the fact that the recorder had a fixed interval of deflection that could only be made smaller or larger through adjustment of the sensitivity. It was suspected that the fixed interval of deflection was a characteristic of the transducer (maximum working range: 0.1 kg; this is the maximum force required to move the cantilever in one direction until the cantilever comes up against the stop) more than of the recorder. In any case, all tetanic recordings deflected to the same maximum point irrespective of where the baseline was chosen. This made it impossible to detect differences (if any) in amplitudes (tensions) as were observed in lower frequency single twitch tracings. A 400-Hz frequency of stimulation, used by Close (1964; 1967), was chosen because a lower frequency of stimulation tended to produce excessively long SOL tetanic contractions, particularly, in control experiments. However, that could have been compacted if the recorder were not already at its lowest chart speed of 0.25 mm/sec. But then again, a lower chart speed, had it been available, would have made such durations as in Figure 12a still less accurate to evaluate. The 400-Hz frequency of stimulation is probably unreasonable for any delicate physiological differences to manifest themselves. Because of these problems, the tetanic recordings may only be discussed on the basis of the

representative tracings for each group.

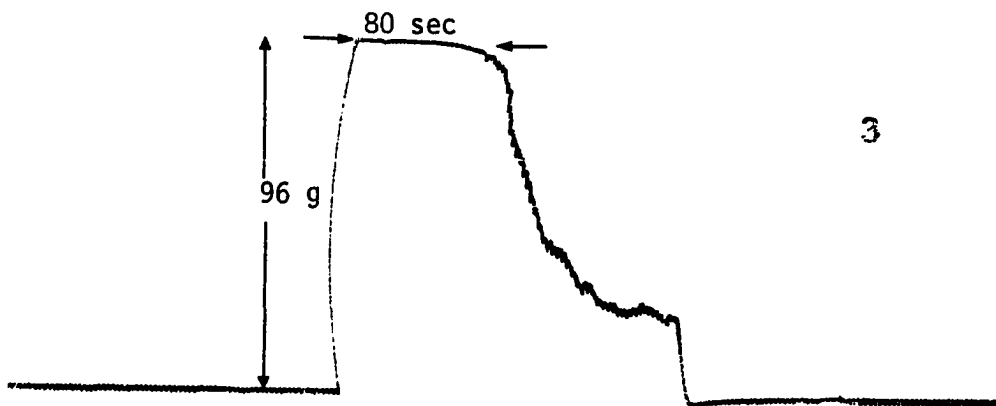
The tetanic tracings show apparent differences in duration between individual indirectly and directly stimulated contractions as well as among all experimental categories of EDL and SOL. An exception to this can be found in the EDL where Figures 9 and 14 (representing CT #1 and MK #4) show no apparent difference (4 sec each) between their respective indirectly and directly provoked durations. No statistics were performed on tetanic recordings because of the erratic nature as well as the wide variability of the tracings. Moreover, some of the tetanic tracings were not suitable for statistical analysis since they had been taken at a time when the animal was either dead or dying.

For CT #1, Figures 9 (EDL) and 15 (SOL) seem to confirm that red muscles (e.g. SOL) do not fatigue as rapidly as the white muscles (e.g. EDL). Observations for CT #2, MK #1, MK #2, MK #3, and MK #4 seem to agree more or less with the observations for CT #1. Since the durations of their indirectly produced tetanic contractions also follow the same pattern as the direct, only to a lesser degree, it is probable that the EDL exhausts its ACh-dependent transmission at the NMJ more quickly than the SOL when the forced frequency of their responses is raised to a value as high as 400 Hz. The phenomenon seemed most pronounced under MK #2 conditions where decreased $[Ca^{++}]$ and increased $[Mg^{++}]$ combined their inhibiting effects to limit the availability of ACh for transmission. But differences in tension values as well as appropriate (less and different) tetanic frequencies of stimulation for each muscle would probably have permitted a more definitive statement that despite its higher

a) Indirect stimulation



b) Direct stimulation

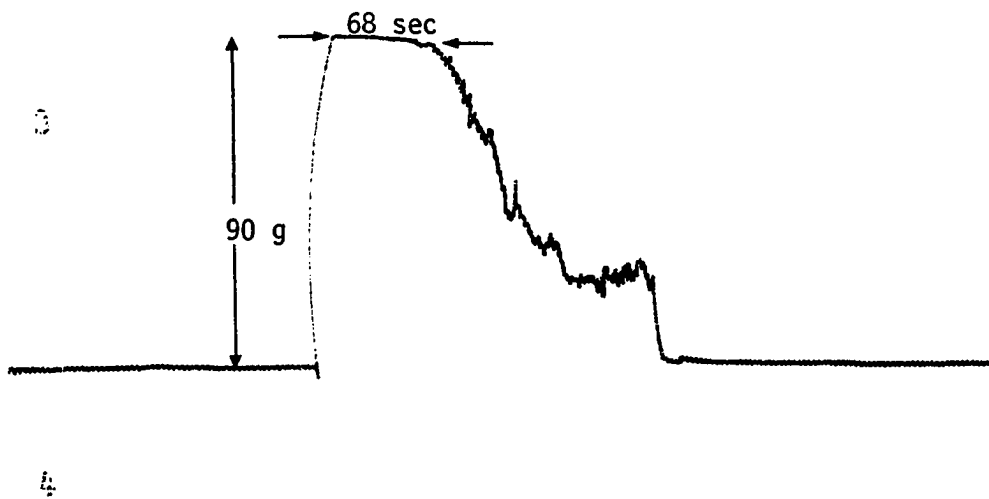


3

4

Figure 9. Sample tetanic tracings from EDL muscle with intact vascular bed

a) Indirect stimulation



b) Direct stimulation

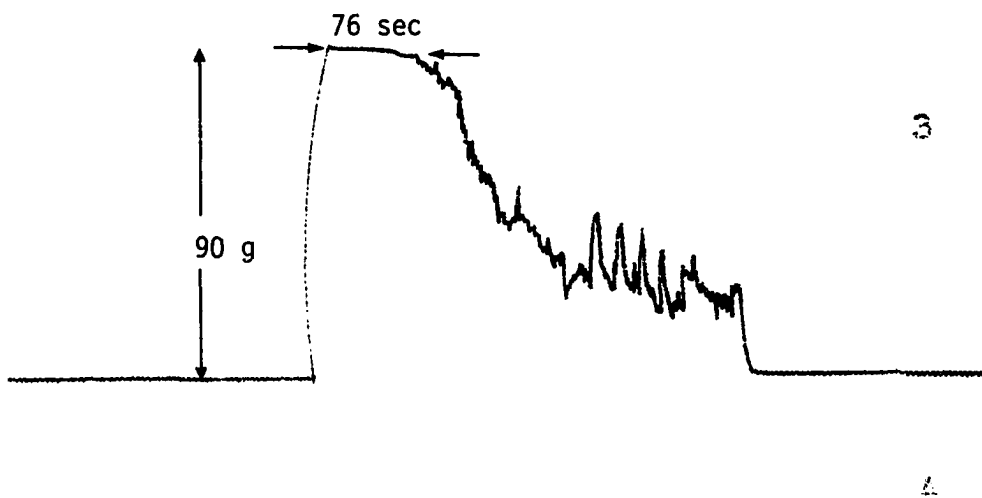
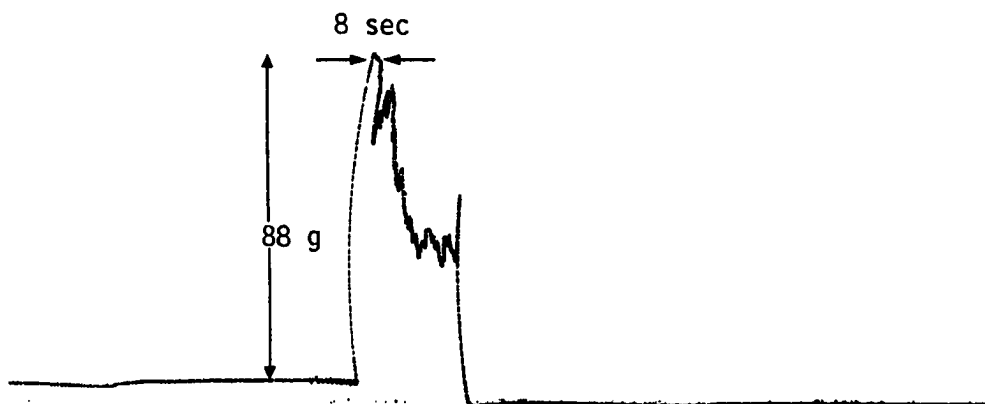


Figure 10. Sample tetanic tracings from EDL muscle perfused with normal Krebs solution

a) Indirect stimulation



b) Direct stimulation

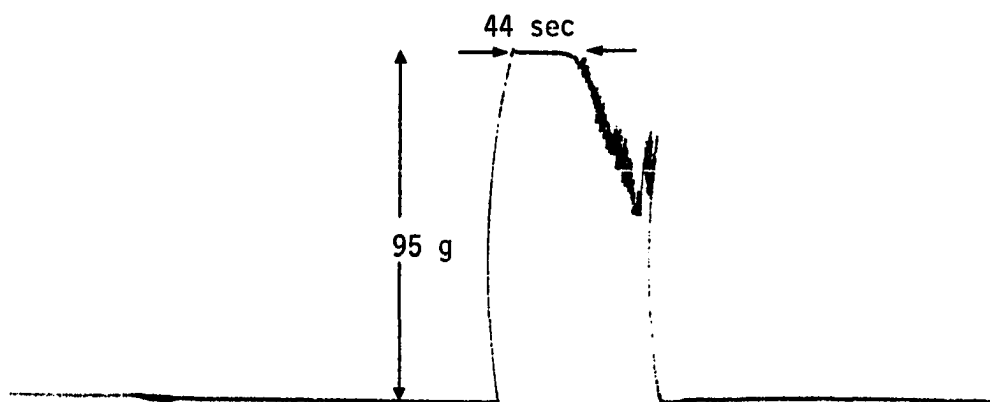
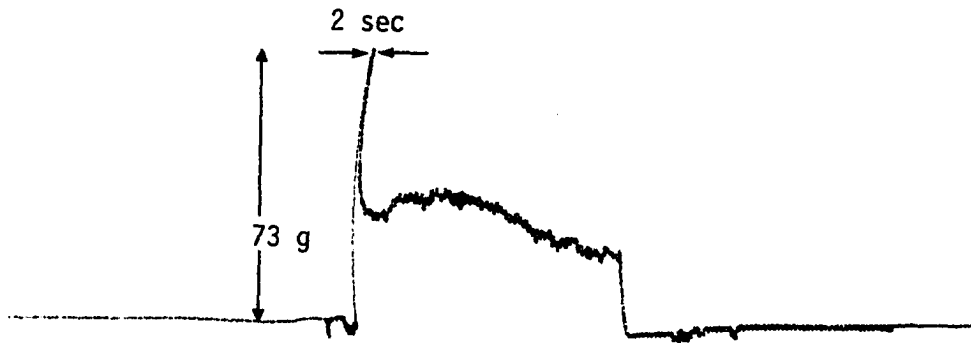


Figure 11. Sample tetanic tracings from EDL muscle perfused with modified Krebs #1

a) Indirect stimulation



b) Direct stimulation

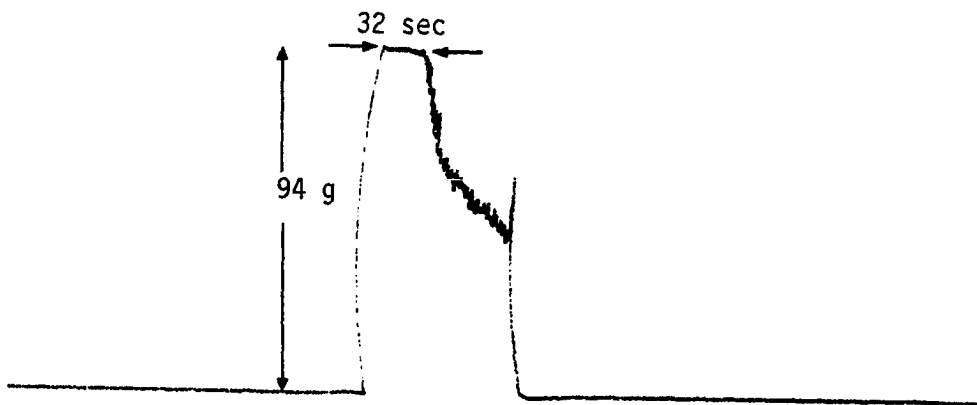
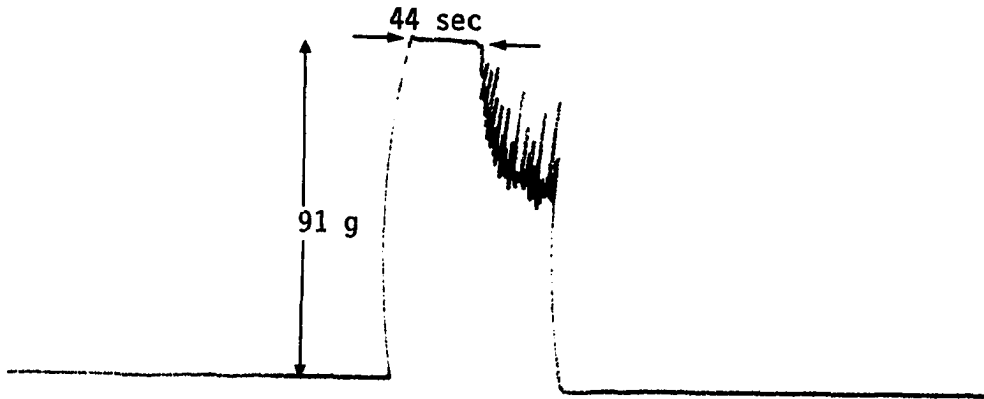


Figure 12. Sample tetanic tracings from EDL muscle perfused with modified Krebs #2

a) Indirect stimulation



b) Direct stimulation

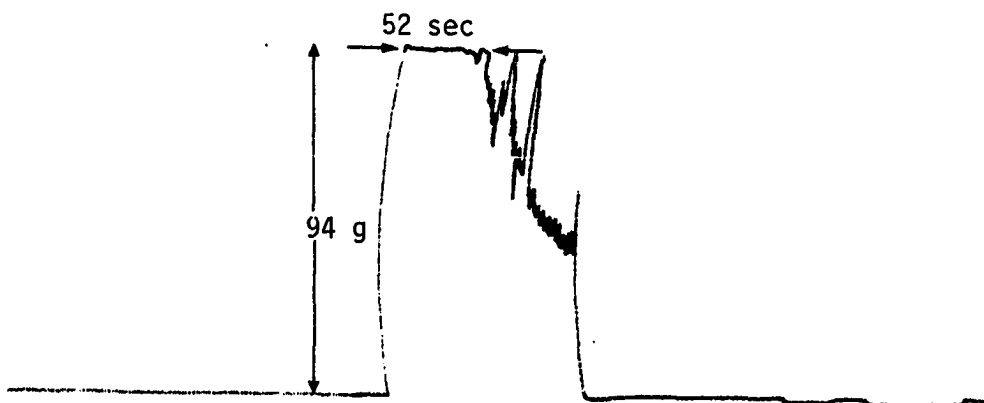
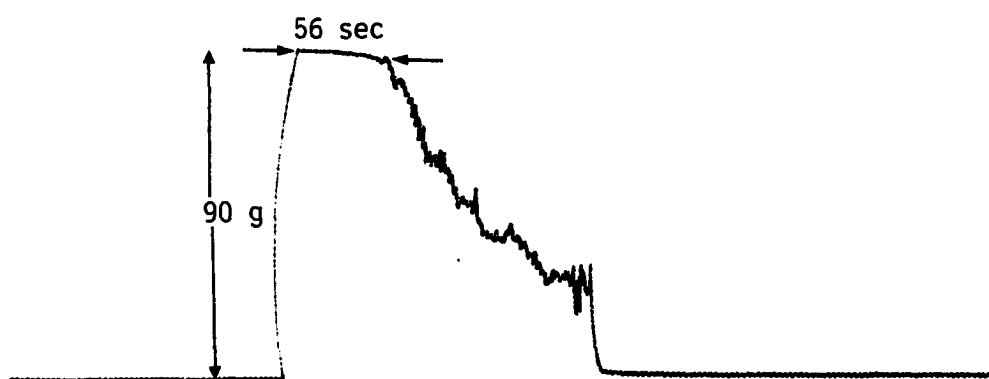


Figure 13. Sample tetanic tracings from EDL muscle perfused with modified Krebs #3

a) Indirect stimulation



b) Direct stimulation

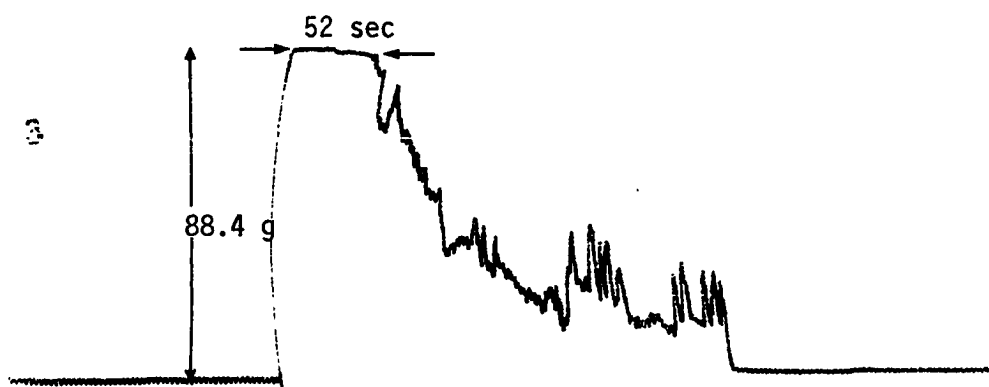


Figure 14. Sample tetanic tracings from EDL muscle perfused with modified Krebs #4

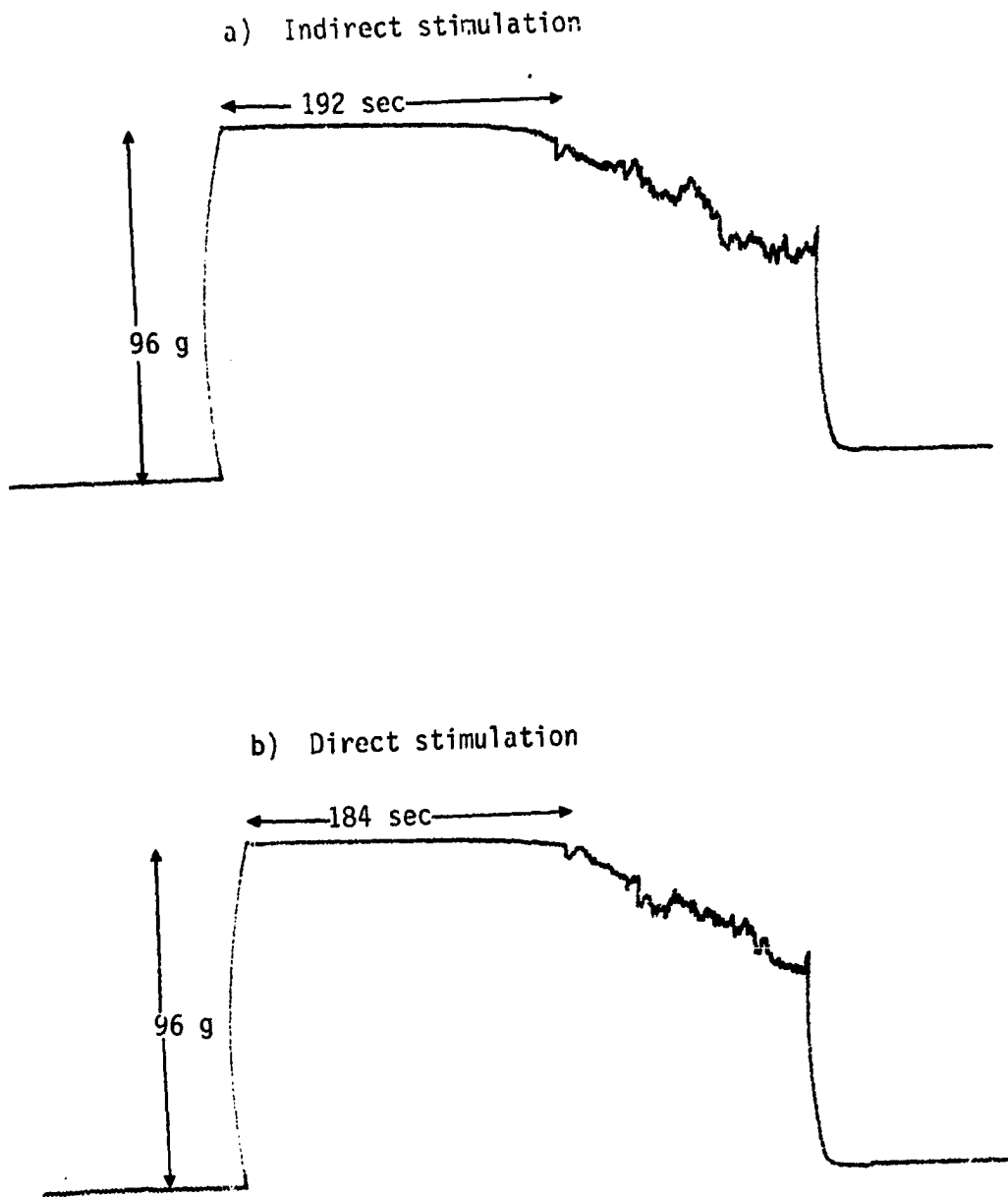


Figure 15. Sample tetanic tracings from SOL muscle with intact vascular bed

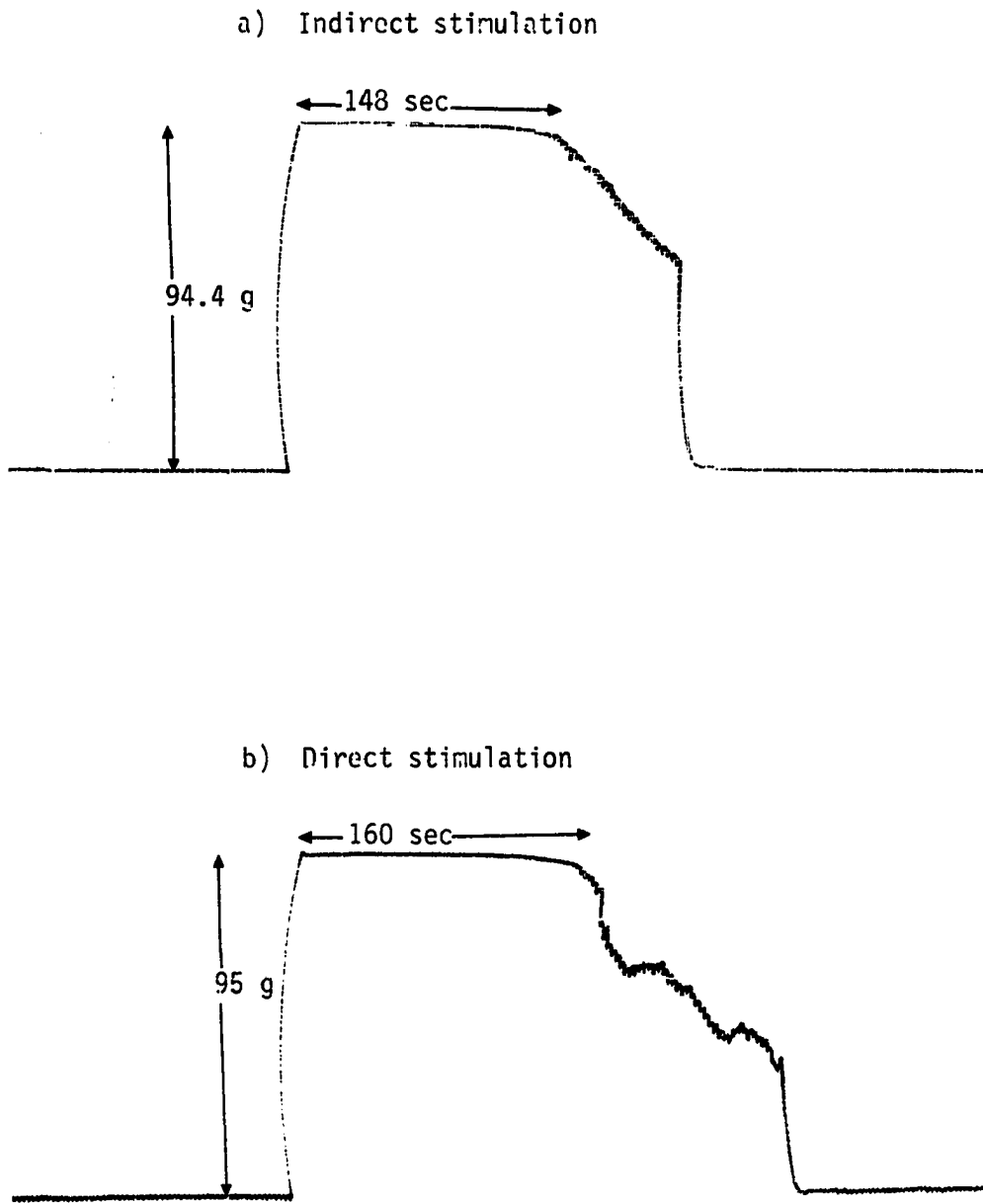
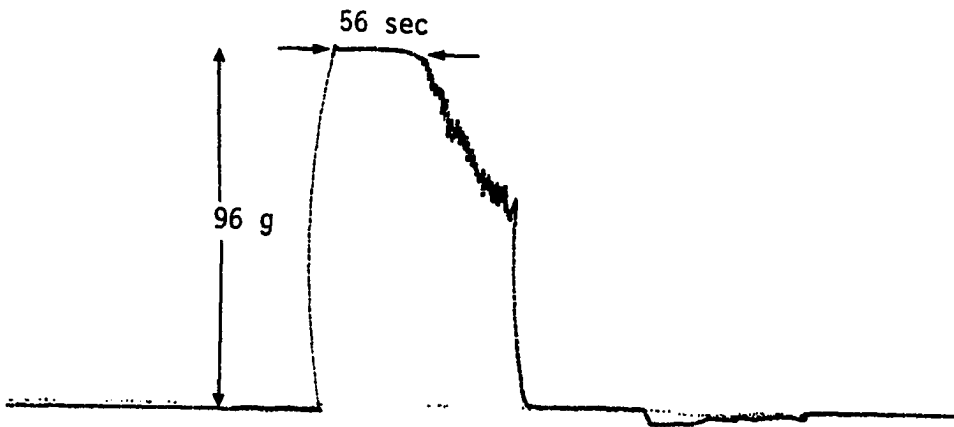


Figure 16. Sample tetanic tracings from SOL muscle perfused with normal Krebs solution

a) Indirect stimulation



b) Direct stimulation

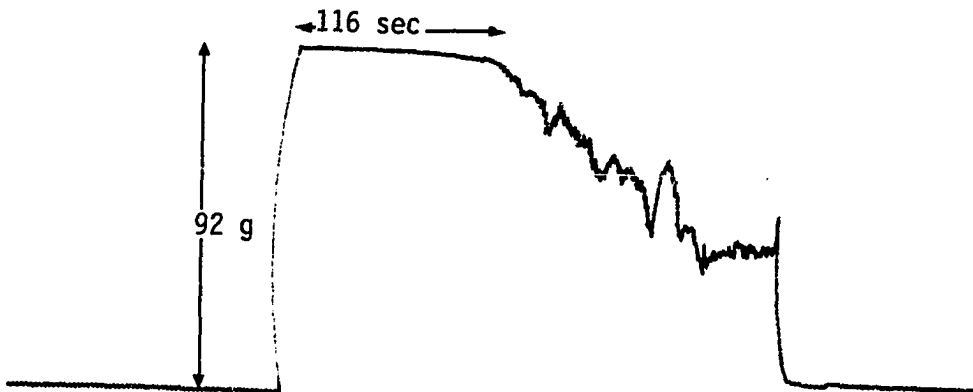
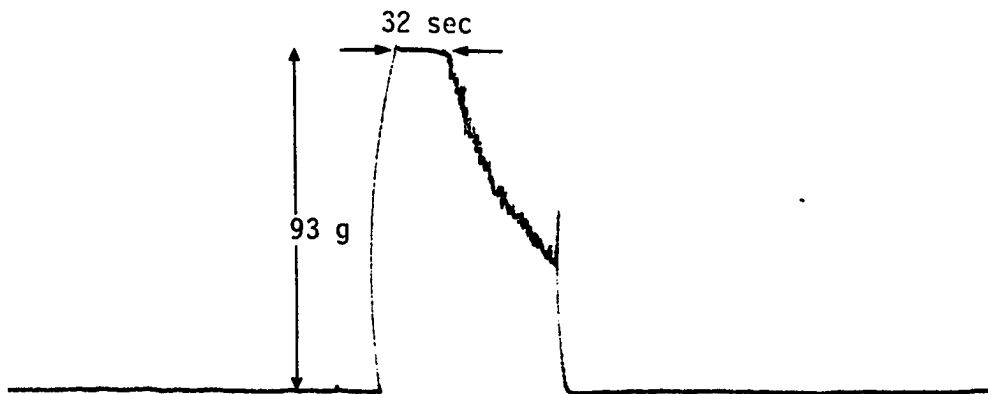


Figure 17. Sample tetanic tracings from SOL muscle perfused with modified Krebs #1

a) Indirect stimulation



b) Direct stimulation

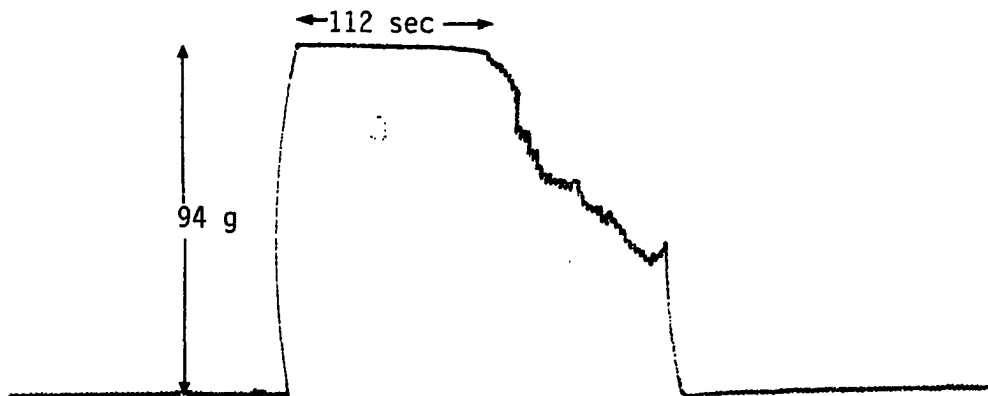


Figure 18. Sample tetanic tracings from SOL muscle perfused with modified Krebs #2

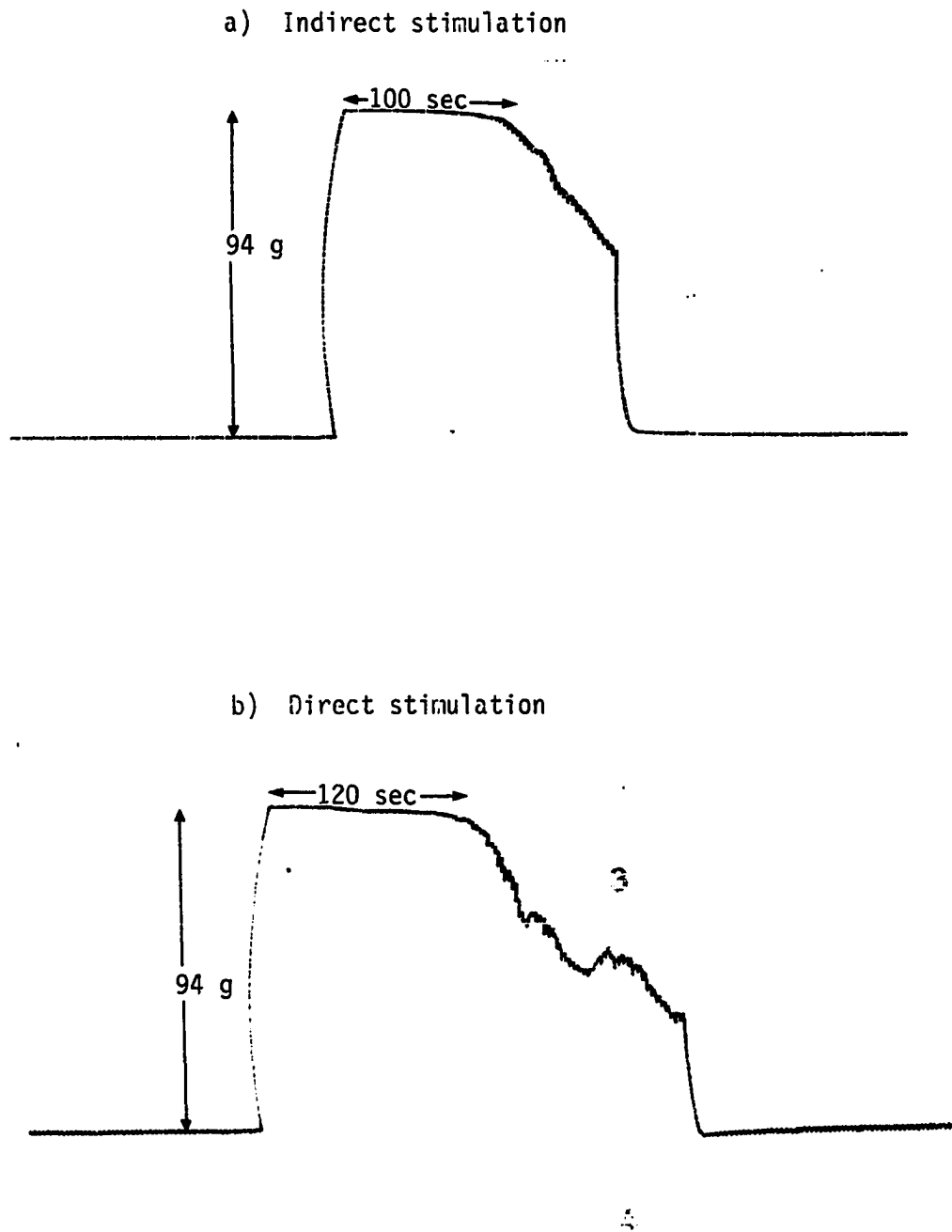


Figure 19. Sample tetanic tracings from SOL muscle perfused with modified Krebs #3

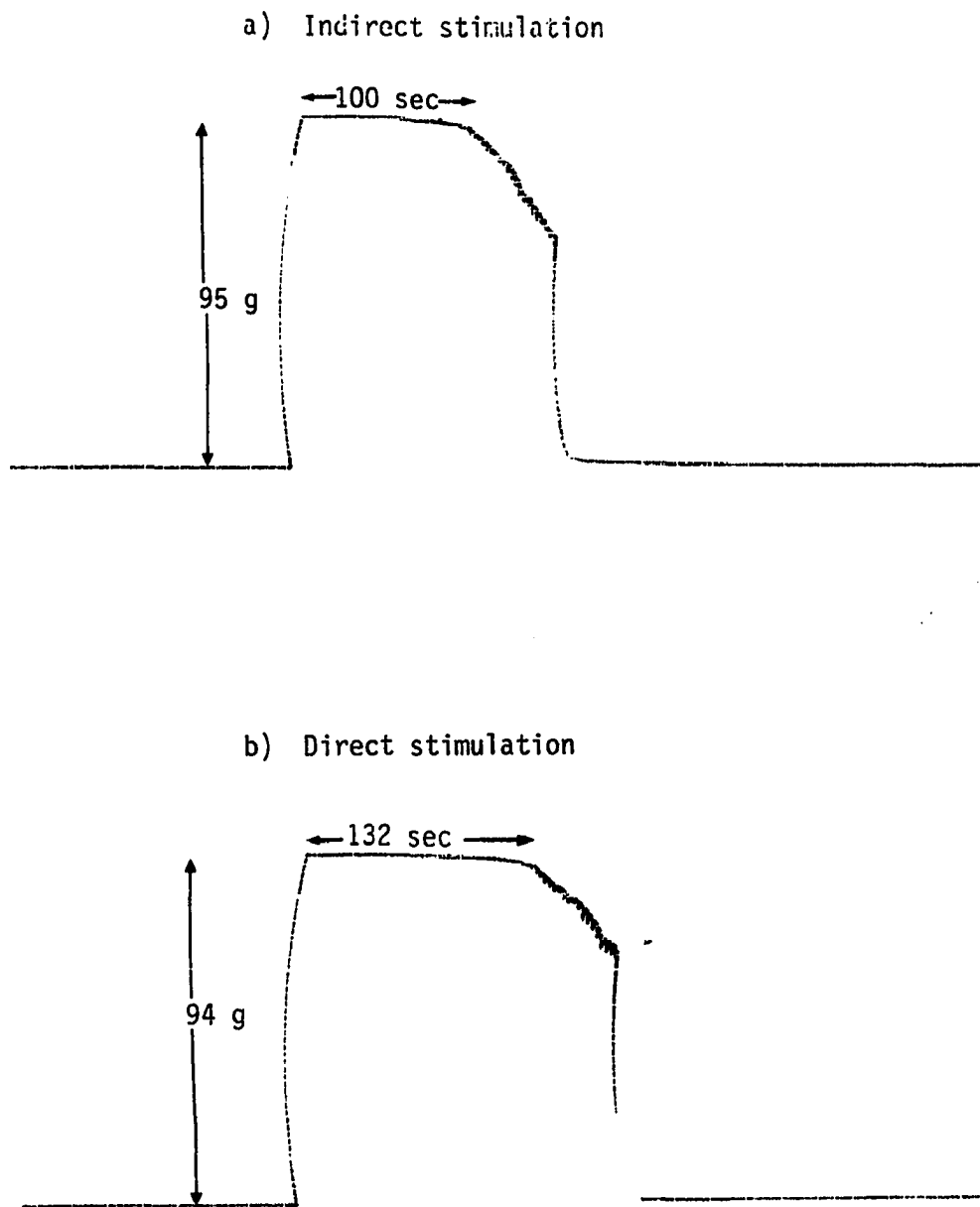


Figure 20. Sample tetanic tracings from SOL muscle perfused with modified Krebs #4

safety factor the EDL, at higher frequencies and at certain ionic concentrations, depletes its ACh reserves faster than the SOL.

Effect of Insulin

Tables 11a and 12a are tabulations of tension observations (in means and their standard deviations) at both T30 (20 min after perfusion starts) and T50 (40 min after perfusion starts) for both EDL and SOL perfused with the five categories of Krebs solution each of which contained 0.5 mg/l of insulin. These tables also contain values for perfusion pressures (PP) and optimal flowrates (FR). Changes in the ionic levels of the influent and effluent "insulinated" Krebs solution have also been listed in Tables 11b and 12b.

The perfusion pressures maintained the same pattern from CT #2 to MK #4 as observed in the major project while flowrates showed no significant change from the predominant optimal value of 6.0 ml/min.

The most obvious insulin effect was the stability it rendered to the nerve-muscle preparation. With insulin in the perfusing Krebs the integrity of the preparation remained long enough to enable recordings to be made at least 40 min (T50) after perfusion was begun. These tracings at T50 were statistically indifferent from those recorded at T30, thus extending the safe recording period to at least 40 min from the start of perfusion (which still had to take place within 10 min of occlusion). The doubling of the recording time eliminates haste and the likelihood of deterioration, both of which could cause an experiment to be terminated, if

Table 11a. Reaction of EDL at 0.4 pps to different [Ca⁺⁺] and [Mg⁺⁺] in Krebs solution containing 0.5 mg/l of insulin

Experiment	PP (mm Hg)	FR (ml/min)	T30		T50	
			Indirect (mN/mm ²)	Direct (mN/mm ²)	Indirect (mN/mm ²)	Direct (mN/mm ²)
Normal Krebs	53.0±1.4	6.1±0.1	56.3±0.8	56.3±0.8	55.3±0.8	56.3±0.8
Modified Krebs #1	47.0±1.4	6.2±0.3	45.3±0.3	55.6±0.4	43.7±0.5	55.4±0.1
Modified Krebs #2	43.0±1.4	6.1±0.1	36.5±0.3	54.8±1.1	36.0±1.0	54.5±0.8
Modified Krebs #3	59.0±1.4	6.0±0.0	51.9±0.5	52.9±2.0	50.1±1.5	51.4±1.1
Modified Krebs #4	50.0±2.8	6.0±0.0	51.0±0.1	51.7±1.1	51.7±1.1	52.2±0.4

Table 11b. Ionic changes in "insulinated" Krebs during EDL perfusion

Experiment	Net gain (+) or loss (-)					
	[Ca ⁺⁺] (mg/dl)	[Mg ⁺⁺] (meq/l)	[P ³⁺] (mg/dl)	[Na ⁺] (meq/l)	[K ⁺] (meq/l)	[Cl ⁻] (meq/l)
Normal Krebs	+0.1	+0.1	+0.7	0.0	+0.5	-7.0
Modified Krebs #1	+0.1	+0.1	+0.6	+2.0	+0.4	-12.0
Modified Krebs #2	+0.3	+0.1	+0.7	+3.0	+0.2	-10.0
Modified Krebs #3	+0.1	---	+0.9	0.0	+0.2	-6.0
Modified Krebs #4	+0.3	---	+1.2	0.0	+0.3	-8.0

Table 12a. Reaction of SOL at 0.1 pps to different [Ca⁺⁺] and [Mg⁺⁺] in Krebs solution containing 0.5 mg/l of insulin

Experiment	PP (mm Hg)	FR (ml/min)	T30		T50	
			Indirect (mN/mm ²)	Direct (mN/mm ²)	Indirect (mN/mm ²)	Direct (mN/mm ²)
Normal Krebs	51.0±1.4	6.1±0.1	28.0±0.3	28.0±0.3	26.9±0.6	27.3±0.9
Modified Krebs #1	49.0±1.7	6.6±0.1	18.1±0.2	26.6±0.7	16.9±0.7	25.8±0.4
Modified Krebs #2	42.0±2.8	6.1±0.1	12.2±0.3	26.1±0.7	11.7±0.0	26.4±0.3
Modified Krebs #3	56.5±2.1	6.7±0.1	26.9±0.6	27.6±0.4	26.0±1.6	26.1±1.7
Modified Krebs #4	50.0±0.0	6.5±0.7	26.3±0.1	27.0±0.8	25.7±1.3	27.0±0.8

Table 12b. Ionic changes in "insulinated" Krebs during SOL perfusion

Experiment	Net gain (+) or loss (-)					
	[Ca ⁺⁺] (mg/dl)	[Mg ⁺⁺] (meq/l)	[P ³⁺] (mg/dl)	[Na ⁺] (meq/l)	[K ⁺] (meq/l)	[Cl ⁻] (meq/l)
Normal Krebs	+0.1	+0.4	+0.7	0.0	+0.5	-7.0
Modified Krebs #1	0.0	-0.1	+0.5	-2.0	+0.3	-14.0
Modified Krebs #2	+0.1	0.0	+0.8	0.0	+0.2	-9.0
Modified Krebs #3	-0.1	---	+0.9	+1.0	+0.3	+2.0
Modified Krebs #4	+0.3	---	+1.3	+1.0	+0.3	-9.0

not influence the results of it.

With insulin, tension values even at T50 were significantly higher than tension values recorded at T30 without insulin, although this evidence is not conclusive since unequal numbers of rats per experiment are being compared. Direct tension values increased by about 21% in the EDL (Table 11a) and about 8% in the SOL (Table 12a) compared to respective ones obtained in the main project (Table 7a: EDL; Table 8a: SOL). Differences among and within the experimental groups with insulin present were insignificant.

Using the same Tables to compare indirect tensions, CT #2 increased by 21% (EDL) and 8% (SOL), MK #1 by 15% (EDL) and 20% (SOL), MK #2 by 19% (EDL) and 33% (SOL), MK #3 by 26% (EDL) and 27% (SOL), and MK #4 by 28% (EDL) and 26% (SOL). Differences among experimental groups for both EDL and SOL were significant except for that between MK #3 and MK #4, and either MK #3 or MK #4 against CT #2. This tends to suggest that the significant differences observed in similar comparisons of CT #2 against MK #3 or MK #4, or MK #3 versus MK #4 in the main experiment might have been due to lack of insulin in the perfusing Krebs solution.

Otherwise, the pattern of changes was very similar to that already observed and discussed in the main experiment, showing that both EDL and SOL react to abnormal concentrations of Ca^{++} and Mg^{++} in their environment but that of the two, SOL is the more sensitive. Also, tetanic contractions and their corresponding durations recorded with insulin in the Krebs solution were similar to those obtained without insulin although it was expected that there would be some difference. Again it is

suspected that the 400-Hz frequency of stimulation must have masked any differences in durations of tetanic contractions that exist between perfusion with and without insulin in the Krebs solution.

Table 13 shows sample values of pH, $p\text{CO}_2$, and $p\text{O}_2$ for the "insulinated" Krebs. The $p\text{O}_2$ difference of 343.5 mm Hg represents a calculated O_2 consumption of 3.12 ml $\text{O}_2/\text{kg}/\text{min}$ for the average hind limb weight of 19.8 g. This is slightly higher than the 2.78 ml $\text{O}_2/\text{kg}/\text{min}$ obtained in the main experiment and could only be attributed to the availability of insulin which consequently facilitated the glucose uptake during the perfusion. The insignificant change between influent and effluent pH as well as the modestly significant change (+2.0 mm Hg) in $p\text{CO}_2$ can be attributed to degeneration of the samples during storage.

Although the main reason for using insulin was its effect on glucose uptake, its effect on extracellular ion concentrations was also of interest. In a recent article, Body et al. (1983) induced hypoglycemia in man through rapid intravenous injection of insulin and observed significant changes in all of the measured variables relating to mineral metabolism. Most striking to them was a 35% decrease in serum inorganic P^{3+} , along with increments in serum total and ionized Ca^{++} and Mg^{++} . These changes were explained on the basis of the known effects of insulin; the hypophosphatemic effect of insulin is thought to represent net movement of P^{3+} from the extracellular compartment to intracellular compartments (Guthmann et al., 1982).

In the insulin studies (Tables 11b and 12b) slight increments were observed in Ca^{++} and Mg^{++} but these had also been observed to about

Table 13. Sample values of pH, pCO₂ and pO₂ for the "insulated" Krebs solution

pH		pCO ₂		pO ₂	
Influent	Effluent	Influent (mm Hg)	Effluent (mm Hg)	Influent (mm Hg)	Effluent (mm Hg)
7.080	7.035	40.3	43.4	481.0	191.7
7.030	7.023	45.9	43.9	594.0	167.8
7.083	7.011	37.3	48.8	495.0	188.6
7.084	6.976	38.0	47.2	439.0	184.6
7.035	7.032	45.2	44.8	597.0	174.8
7.071	7.040	50.6	46.8	569.0	194.0
7.092	6.975	37.4	53.0	505.0	180.8
7.094	7.329	36.5	27.1	491.0	164.2
7.089	7.077	37.3	49.4	461.0	90.7
7.101	7.315	36.4	20.1	504.0	163.6
7.076 _{-0.02}	7.081 _{+0.13}	40.5 _{+5.0}	42.5 _{+10.5}	513.6 _{+54.7}	170.1 _{+30.0}

the same degree in the main study where insulin was not a factor. A slight net gain in P^{3+} instead of a loss as reported by Body et al. (1983) was also observed, but the gain with insulin was much less than the gain without insulin.

CONCLUSIONS

The project succeeded in determining that differences in nerve, muscle, and neuromuscular junction (NMJ) do indeed result in varying responses to abnormal concentrations of Ca^{++} and Mg^{++} .

Using normal and altered $[\text{Ca}^{++}]$ and $[\text{Mg}^{++}]$ to perfuse both SOL and EDL neuromuscular systems, and comparing their respective isometric tensions, it was possible to deduce that the known differences in safety factor and normal activity patterns of slow (SOL) and fast (EDL) twitch muscles result in different responses to altered ionic concentrations.

In control #1 experiments, the similar amplitudes of both indirectly and directly stimulated twitches indicated that the indirect and direct stimulus voltages caused all motor units of either EDL or SOL to fire. Since tensions obtained while perfusing with normal Krebs solution (CT #2) were about 75% of the tensions recorded in intact animals, changes due to the subsequent ionic modifications in the solution were conspicuous enough to prove the hypothesis.

In MK #1 (decreased $[\text{Ca}^{++}]$, normal $[\text{Mg}^{++}]$) the observed indirect stimulation twitches showed statistically significant depreciation in contrast to direct stimulation twitches which were statistically indif-ferent from the direct stimulation twitches of CT #2. The occurrence showed clearly that Ca^{++} insufficiency had interfered with the capacity to activate the normal amount of ACh release required to invoke all NMJs to produce suprathreshold EPPs. The consequent fewer MAPs ultimately caused fewer muscle cells to contract, yielding an amplitude far smaller

than that from direct stimulation. Of the two systems, SOL NMJ showed significantly greater sensitivity to Ca^{++} insufficiency than its EDL NMJ counterpart.

In MK #2 the synergistic effects of low $[\text{Ca}^{++}]$ and high $[\text{Mg}^{++}]$ in blocking ACh release at the NMJ caused more reduced indirect stimulation tensions compared to what low $[\text{Ca}^{++}]$ alone had produced in MK #1. Although both EDL and SOL NMJs reacted to the effects of low $[\text{Ca}^{++}]$ and high $[\text{Mg}^{++}]$, the SOL NMJ was more sensitive than the EDL NMJ.

The reactions of MK #3 and MK #4 were unexpected. In both EDL and SOL the low Mg^{++} in MK #3 caused significant (indirectly stimulated) twitch depreciations. MK #3 was expected to produce the same results as CT #2 since theoretically low Mg^{++} should be causing more than normal amounts of ACh to reach the endplate. The still greater depreciation observed in MK #4 must have been brought on by an overriding low Ca^{++} effect since low Ca^{++} caused reduction in indirectly provoked twitches in MK #1. In both MK #3 and MK #4 SOL NMJ again seemed to have showed greater reaction to the modifications in the Krebs solution. It is possible that these effects are due to poor glucose utilization since they seem to disappear in the presence of insulin.

In summary, for single twitches the EDL NMS showed less sensitivity to changes in $[\text{Ca}^{++}]$ and $[\text{Mg}^{++}]$ than the SOL, implying that at certain $[\text{Ca}^{++}]_e$ and $[\text{Mg}^{++}]_e$, transmission could be maintained in EDL but not in SOL.

The transducer used in this project was not suitable for tetanic tracings where amplitude variations were sought. Also, the 400-Hz

frequency of stimulation was too high for delicate physiological differences to manifest themselves. However, the respective durations of the EDL and SOL tetanic contractions that were recorded seemed to indicate that despite its higher safety factor, the EDL NMJ at higher frequencies and at certain ionic concentrations is more susceptible to failure than the SOL NMJ.

Further experiments using normal and modified Krebs solutions containing insulin and normal physiological frequencies of stimulation are needed to determine which of these two neuromuscular systems is more sensitive to known pathological conditions of altered $[Ca^{++}]$ and $[Mg^{++}]$.

BIBLIOGRAPHY

- Andrew, B. K. and N. J. Part. 1972. Properties of fast and slow motor units in hind limb and tail muscles of the rat. *J. Exp. Physiol.* 57:213-225.
- Body, J. J., P. E. Cryer, K. P. Offord, and H. Heath III. 1983. Epinephrine is a hypophosphatemic hormone in man: Physiological effects of circulating epinephrine on plasma calcium, magnesium, phosphorus, parathyroid hormone, and calcitonin. *J. Clin. Invest.* 71:572-578.
- Bowen, J. M., D. M. Blackmon, and J. E. Heavner. 1970. Neuromuscular transmission and hypocalcaemic paresis in the cow. *Am. J. Vet. Res.* 31:831-839.
- Buchthal, F. and H. Schmalbruch. 1970. Contraction times and fiber types in intact human muscles. *Acta Physiol. Scand.* 79:435-452.
- Buchthal, F. and H. Schmalbruch. 1980. Motor unit of mammalian muscle. *Physiol. Rev.* 60(1):90-142.
- Buchthal, F., K. Dahl, and P. Rosenfalck. 1973. Risettime of the spike potential in fast and slowly contracting muscles of man. *Acta Physiol. Scand.* 87:261-269.
- Buller, A. J., J. C. Eccles, and R. Eccles. 1960. Differentiation of fast and slow muscles in the cat hind limb. *J. Physiol.* 150:399-416.
- Buller, A. J., D. M. Lewis, and R. M. Ridge. 1965. Some electrical characteristics of fast twitch and slow twitch skeletal muscle fibers in the cat. *J. Physiol. London* 180:29-30.
- Close, R. I. 1964. Dynamic properties of fast and slow skeletal muscles of rat during development. *J. Physiol.* 173:74-95.
- Close, R. I. 1967. Properties of motor units in fast and slow skeletal muscles of the rat. *J. Physiol.* 193:45-55.
- Close, R. I. 1972. Dynamic properties of mammalian skeletal muscles. *Physiol. Rev.* 52(1):129-197.
- Close, R. I. and J. F. Hoh. 1968. Influence of temperature on isometric contractions of rat skeletal muscles. *Nature London* 217:1179-1180.

- Darrah, M. I. 1982. Physiological effects of blood flow through a region of induced atherosclerosis in the rat with emphasis on the effect of exercise on thrombosis and collateral vessel recruitment. Ph.D. Thesis. Iowa State University, Ames, Iowa.
- Ebashi, S. and M. Endo. 1968. Calcium ions and muscles contraction. *Progr. Biophys.* 18:123-183.
- Ebashi, S., M. Endo, and I. Ohtsuki. 1969. Control of muscle contraction. *Quart. Rev. Biophys.* 2:351-384.
- Eccles, J. C., R. M. Eccles, and A. Lundberg. 1958. The action potentials of the alpha motorneurons supplying fast and slow muscles. *J. Physiol. London* 142:275.
- Eccles, J. C. and C. S. Sherrington. 1930. Numbers and contraction values of individual motor units examined in some muscles of the limb. *Proc. Roy. Soc. Ser. Biol. Sci.* 106:326.
- Ellisman, M. H., J. E. Rash, A. Staehelin, and K. R. Porter. 1976. A comparison of specializations at neuromuscular junctions and non-junctional sarcolemmas of mammalian fast and slow twitch muscle fibers. *J. Cell Biol.* 68:752-774.
- Erulkar, S. D. and Alan Fine. 1979. Calcium in the nervous system. *Rev. of Neurosc.* 4:179-232.
- Folkow, B. and H. D. Halicka. 1968. A comparison between "red" and "white" muscles with respect to blood supply, capillary surface area and oxygen uptake during rest and exercise. *Microvasc. Res.* 1:1-14.
- Frankenhaeuser, B. 1957. The effect of calcium on the myelinated nerve fiber. *J. Physiol.* 137:245-269.
- Gaddum, J. H., K. A. Hameed, D. E. Hathway, and F. F. Stephens. 1955. Quantitative studied of antagonists for 5-hydroxytryptamine. *Q. J. Exp. Physiol.* 40:49-74.
- Ganong, W. F. 1977a. Circulation through special regions. Page 453 in *Review of Medical Physiology*. 8th ed. Lange Publications, Los Altos, California.
- Ganong, W. F. 1977b. Gas transport between the lungs and the tissues. Page 495 in *Review of Medical Physiology*. 8th ed. Lange Publications, Los Altos, California.
- Gasser, H. S. and H. Grundfest. 1939. Axons diameters in relation to

the spike dimensions and the conduction velocity of the mammalian A fiber. *Amer. J. Physiol.* 127:393.

- Gertler, R. A. and N. Robbins. 1978. Differences in neuromuscular transmission in the red and white muscles. *Brain Res.* 142:160-164.
- Guthmann, H. M., G. M. Palmieri, A. B. Hinton, and A. L. Guthmann. 1982. The mechanism of insulin-induced hypercalcaemia in the chick. *Endocrinology* 110:571-574.
- Hanson, J. 1974. The effects of repetitive stimulation on the action potential and the twitch of rat muscle. *Acta Physiol. Scand.* 90:387-400.
- Henneman, E., G. Somjen, and D. O. Carpenter. 1965. Excitability and inhibitability of motoneurons of different sizes. *J. Neurophysiol.* 28:599.
- Hilton, S. M. and G. Vrbova. 1968. Absence of functional hyperaemia in the slow muscle of the cat. *J. Physiol.* 194:86-87.
- Hilton, S. M., M. G. Jeffries, and G. Vrbova. 1970. Functional specialization of the vascular bed of the soleus muscle. *J. Physiol.* 206:543-562.
- Hubbard, J. I. 1973. Microphysiology of vertebrate neuromuscular transmission. *Physiol. Review* 53:674-723.
- Huxley, A. F. 1974. Muscular contraction. *J. Physiol.* 243:1.
- Jenkinson, D. H. 1957. The nature of the antagonism between calcium and magnesium ions at the neuromuscular junction. *J. Physiol.* 138:434-444.
- Jewell, P. A. and E. J. Zaimis. 1954. A differentiation between red and white muscle in the cat based on responses to neuromuscular blocking agents. *J. Physiol.* 124:417-428.
- Katz, B. 1971. Quantal mechanism of neural transmitter release. *Science* 173:123.
- Katz, B. and R. Miledi. 1965. The effect of calcium on acetylcholine release from motor nerve terminals. *Proc. R. Soc. B.* 161:495-503.
- Katz, B. and R. Miledi. 1967a. A study of synaptic transmission in the absence of nerve impulses. *J. Physiol.* 192:407-436.
- Katz, B. and R. Miledi. 1967b. The release of acetylcholine from nerve by graded electric pulses. *Proc. R. Soc. B.* 167:23-38.

- Katz, B. and R. Miledi. 1967c. The timing of calcium action during neuromuscular transmission. *J. Physiol.* 189:535-544.
- Katz, B. and R. Miledi. 1969. Tetrodotoxin resistant electric activity in presynaptic terminals. *J. Physiol.* 203:459-487.
- Kullberg, R. W., T. L. Lentz, and M. V. Cohen. 1977. Development of the myotomal neuromuscular junction in *Xenopus laevis*: An electrophysiological and fine structural study. *Dev. Biol.* 60:101-130.
- Lester, H. A. 1977. The response to acetylcholine. *Sci. Am.* 236:106.
- Llinas, R. and C. Nicholson. 1975. Calcium role in depolarization-secretion coupling, an aequorin study in giant synapse. *Proc. Nat. Acad. Sci.* 72:187-190.
- Luff, A. R. and H. L. Atwood. 1971. Changes in the sarcoplasmic reticulum and transverse tubular system of fast and slow skeletal muscles of the mouse during postnatal development. *J. Cell Biol.* 51:369-383.
- Miledi, R. 1973. Transmitter release induced by injection of calcium ions into nerve terminals. *Proc. R. Soc. B.* 183:421-425.
- Miledi, R. and J. Zelena. 1966. Sensitivity to acetylcholine in rat slow muscle. *Nature London* 210:855-856.
- Nastuk, W. L. and J. H. Liu. 1966. Muscle postjunctional membrane: Changes in chemosensitivity produced by calcium. *Sci.* 154:266-267.
- Nelson, L. S. 1960. Hypocalcaemia in cattle. *J. A. V. M.* 137:705-709.
- Padykula, H. A. and G. F. Gauthier. 1967. Morphological and cytochemical characteristics of fiber types in normal mammalian skeletal muscle. Pages 117-128 in A. T. Milhorat, ed. *Exploratory Concepts in Muscular Dystrophy and Related Disorders*. Excerpta Med. Found., Amsterdam.
- Padykula, H. A. and G. F. Gauthier. 1970. The ultrastructure of the neuromuscular junctions of mammalian red, white, and intermediate skeletal muscle fibers. *J. Cell Biol.* 46:27-41.
- Paton, W. D. M. and E. J. Zaimis. 1951. The action of d-Tubocurarine and decamethonium on respiratory and other muscles in the cat. *J. Physiol.* 112:311-331.

- Paton, W. D. M. and D. R. Waud. 1967. The margin of safety of neuromuscular transmission. *J. Physiol.* 191:59-90.
- Rahamimoff, R. 1976. The role of calcium in transmitter release at the neuromuscular junction. Pages 117-149 in S. Thesleff, ed. *Motor Innervation of Muscle*. Academic Press, New York.
- Ranvier, L. 1873. Proprietes et structures differentes des muscles rouges et des muscles blancs chez les raies. *C. R. Acad. Sci.* 77: 1030-1034.
- Resnick, S. 1964. Hypocalcaemic tetany in the dog. *J. A. V. M.* 144: 1115-1118.
- Salpeter, M. M. 1967. The distribution of acetylcholinesterase at motor endplates of a vertebrate twitch muscle. *J. Cell Biol.* 32:379.
- Stainsby, W. N. 1973. Local control of regional blood flow. *Ann. Rev. Physiol.* 35:151.
- Stowe, C. M. 1965. Ganglionic blocking and muscle relaxant drugs. Pages 336-340 in L. M. Joves, ed. *Veterinary Pharmacology and Therapeutics*. 3rd ed. Iowa State University Press, Ames, Iowa.
- Takeuchi, N. 1963. Effects of calcium on the conductance change of the endplate membrane during the action of transmitter. *J. Physiol.* 167:141-155.
- Thomas, R. S. and J. W. Greenanwalt. 1968. Microincineration, electron microscopy, and electron diffraction of calcium phosphate-loaded mitochondria. *J. Cell Biol.* 39:55.
- Voisin, A. 1963. *Grass tetany*. Charles Thomas Publisher, Springfield, Illinois.

ACKNOWLEDGEMENTS

I am not sure that I know what the acquisition of a Ph.D. means to other scholars. What I know for sure, however, is that for me, a personal dream has come true. Thus no amount of thanks can express my gratitude to Dr. Mary Helen Greer who has fully participated in my quest for this level of intellectual growth.

I also wish to acknowledge, most heartily, the numerous pieces of invaluable advice and suggestions of Dr. W. H. Brockman, Dr. Pam MacAllister, Dr. F. Hembrough, Dr. E. T. Littledike, Dr. R. W. Carithers and Dr. Mark Darrah.

My gratitude goes wholeheartedly to both academic and administrative staff of Biomedical Engineering Department for the opportunity and the financial support.

Finally, I thank my wife and children for their patience.

NOTES